



SATHYABAMA

INSTITUTE OF SCIENCE AND TECHNOLOGY
(DEEMED TO BE UNIVERSITY)

Accredited "A" Grade by NAAC | 12B Status by UGC | Approved by AICTE

www.sathyabama.ac.in

School of Mechanical
Department of Aeronautical Engineering

UNIT – I - SAE1305 EXPERIMENTAL AERODYNAMICS

1.0 Introduction

Need of experiments

(i) Theory is incomplete and needs to be supplemented.

(ii) Information of fundamental nature needed in many areas.

Experimental information towards solving aerodynamic problems could be obtained in a number of ways. Flight tests, rocket flights, drop tests water tunnels, ballistic ranges and wind tunnels are some of the ways by which aerodynamic data can be generated. With the help of well performed experiments even information of fundamental nature could be derived.

Wind tunnel

Majority of experimental data needed in aerodynamics is generated using wind tunnels. Wind Tunnel is a device for producing airflow relative to the body under test. Wind tunnels provide uniform flow conditions in their test section.

1.1 Classification of wind tunnels

Wind tunnels may be classified based on any of the following:

(a) Speed, Mach no

They are classified as of low speed or high speed wind tunnels .In wind tunnel parlance, high speed wind tunnels are those operating at speeds where compressibility effects are important. They are also classified based on the Mach number of operation as subsonic, transonic, supersonic or hypersonic wind tunnels.

(b) Mode of operation (Pressure storage, in-draft or Pressure vacuum type.)

(c) Kind of test section (T.S) - Open, Closed or Semi enclosed

1.2 Applications of wind tunnels

1. *Aerodynamic applications*
2. *Non-Aero applications in*
 - Civil Engineering
 - Automobile Engineering
 - Calibration of instruments

1.3 Model making, Non-dimensional parameters

Geometric similarity

One of the most important requirements of models is that there should be geometric similarity between the model and the prototype. By geometric similarity it is meant that ratios of corresponding dimensions in the model and the prototype should be the same.

Dynamic similarity

Equally important as the geometric similarity is the requirement of dynamic similarity. In an actual flight, when the body moves through a medium, forces and moments are generated because of the viscosity of the medium and also due to its inertia, elasticity and gravity. The inertia, viscous, gravity and elastic forces generated on the body in flight can be expressed in terms of fundamental units. The important force ratios can be expressed as non dimensional numbers. For example,

- Reynolds number (Re) = Inertia force/Viscous force
- Mach number = Inertia force/Elastic force
- Froude number = Inertia force/Gravity force

The principle of dynamic similarity is that a scale model under same Reynolds number and Mach number will have forces and moments on it that can be scaled directly. The flow patterns on the full scale body and the model will be exactly similar.

It is not necessary and may not be possible that all the aforesaid non dimensional numbers be simulated simultaneously in any experiment. Depending on the flow regime or the type of experiments, certain non-dimensional parameters are important. For example, in a low speed flow regime, simulation of Reynolds number in the experiments is important to depict the conditions of actual flight. In a high speed flow, simulation of Mach number is significant. It may even be necessary and significant that more than one non dimensional parameter are simulated. The principle of dynamic similarity is applicable in other fields of engineering too.

As examples:

Stanton number is simulated in heat transfer experimentation.

Stanton no (St) = Heat transferred in to the fluid / Thermal capacity

$$St = \frac{h}{c_p \rho v}$$

where h =convective heat transfer coefficient

ρ = density

c_p = specific heat at constant pressure

v = velocity

Expressing in terms of non-dimensional parameters,

$$St = \frac{Nu}{Re * Pr}$$

$$St = \frac{q}{\rho c_p (T_0 - T_w)}$$

Strouhal number is used in experiments dealing with oscillating flow

$$S = \frac{f_s l}{u}$$

f_s is vortex shedding frequency,

l is the characteristic length and

v the velocity

Knudsen number $\text{Kn} = \frac{\lambda}{l}$ is simulated in low density flows.

In the definition above, λ is the mean free path and l the characteristic dimension.



SATHYABAMA

INSTITUTE OF SCIENCE AND TECHNOLOGY
(DEEMED TO BE UNIVERSITY)

Accredited "A" Grade by NAAC | 12B Status by UGC | Approved by AICTE

www.sathyabama.ac.in

School of Mechanical
Department of Aeronautical Engineering

UNIT – II - SAE1305 EXPERIMENTAL AERODYNAMICS

SAE1305 EXPERIMENTAL AERODYNAMICS

UNIT 2 LOW SPEED WIND TUNNEL

1.0 Low speed wind tunnel

Low speed wind tunnels may be of open circuit or closed circuit.

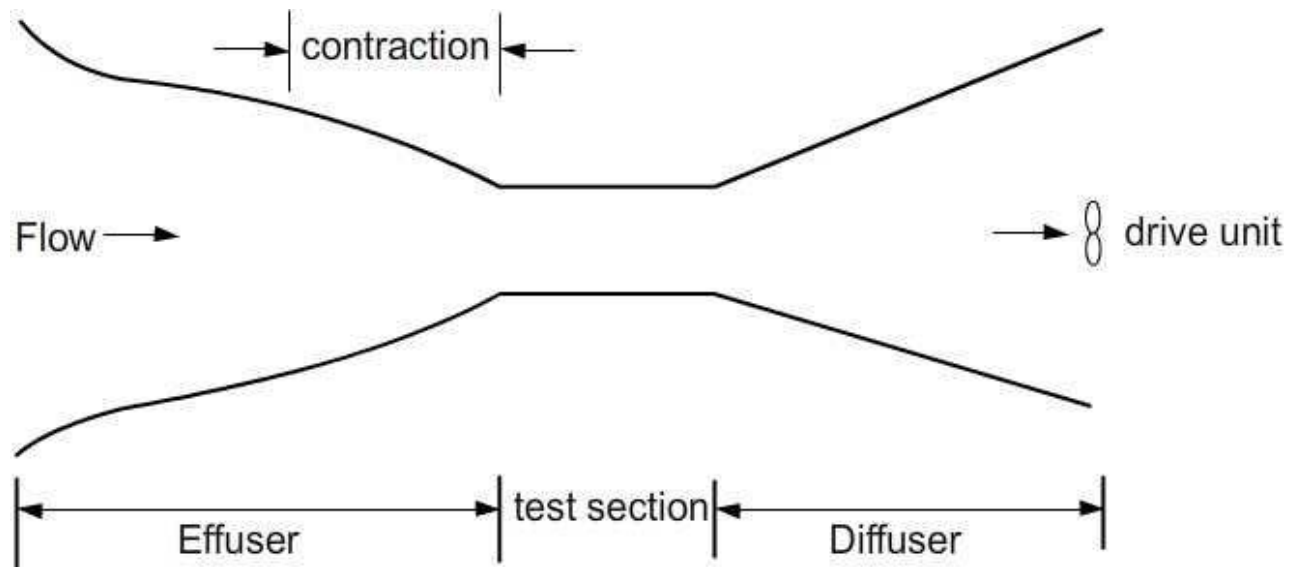
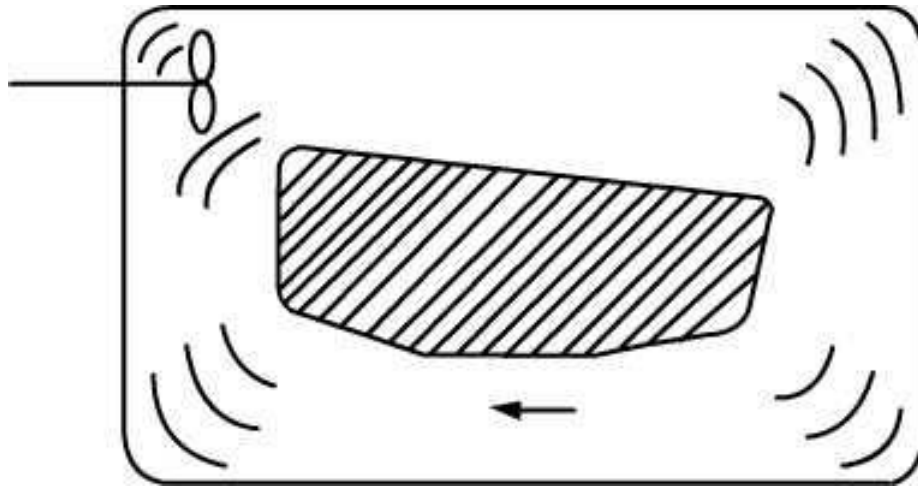


Figure 1.1 Schematic of an open circuit low speed wind tunnel

Figure 1.1 shows an open circuit low speed wind tunnel. After each run, the intake gets air fresh from the atmosphere. The effuser of the wind tunnel is the part of the wind tunnel from the beginning to the entry to the test section. The effuser makes the flow ready for the test section conditions. The test section provides the desired uniform flow conditions along and across the section. It is important that the test section conditions are controllable. Figure 1.2 shows a closed circuit wind tunnel. Losses in vorticity, eddies and turbulence are unavoidable in the tunnel circuit. If velocity is large, skin friction and losses due to obstacles will be correspondingly large.



**Figure 1.2 Schematic of an open circuit
low speed wind tunnel**

1.1 Irregularities of flow in low speed tunnels

- 1) Spatial non uniformity → Mean velocity not be uniform over a cross section. This is overcome by transferring excess total head from regions of high velocity to those of low velocity.
- 2) Swirl → Flow may rotate about an axis resulting in variation of direction of flow. Flow straighteners and honey combs are used to reduce swirl.
- 3) Low frequency pulsation → These are surges of mean velocity. Under their influence, time taken for steady conditions becomes excessive. It is difficult to locate the source of such pulsations.
- 4) Turbulence → Turbulence generates small eddies of varying size and intensity and results in time variations of velocity. Turbulence may be defined as irregular fluctuations of velocity superimposed on mean flow.

In order to quantify turbulence:

Take components of mean velocity as U, V, W

Those of turbulent velocity u, v, w

RMS values $\sqrt{(\bar{u})^2}$, $\sqrt{(\bar{v})^2}$ and $\sqrt{(\bar{w})^2}$ are denoted as u', v', w'

Intensity of turbulence = $\frac{u'}{V_0}$ or $\frac{v'}{V_0}$ or $\frac{w'}{V_0}$ where, V_0 is the mean of U, V, W

Scale of turbulence $L = \int_0^{\infty} R_y \, dy$

where R is the coefficient of co-relation between the longitudinal component of turbulent velocity at A and that at another point B distant y from it.

$$R_y = \frac{\overline{u_A u_B}}{u'_A u'_B}$$

1.2 Reduction of turbulence

Effect of screens on turbulence

Use of wire meshes (also called as gauzes or screens) is very common. Screens of very fine mesh size are used. They are kept as far upstream of the test section as possible. Screens are usually made of metal, nylon or polyester. With the use of screens, larger eddies are broken down to smaller ones and the smaller ones decay rapidly. Multiple screens reduce turbulence intensity.

The scale of eddies depends on the flow Re based on wire diameter of the flow through the screens. The eddies are practically absent when the Re is < 40 . One of the important reasons for keeping the screens at the beginning of the tunnel circuit is to ensure that they are at the low velocity regions where the Re is the least. Effect of screen on turbulence depends on K, the pressure drop coefficient.

$$K = \frac{p_1 - p_2}{1/2 \rho v_1^2}$$

where p_1 and p_2 are values of pressure up and downstream of the screen. K depends also on β , Re, θ . Re the Reynolds number and θ is the flow incidence angle measured from normal to the screen

β is the open area ratio and is defined as $\beta = \left(1 - \frac{d}{l}\right)^2$ 'l' and 'd' are marked on Figure 2.

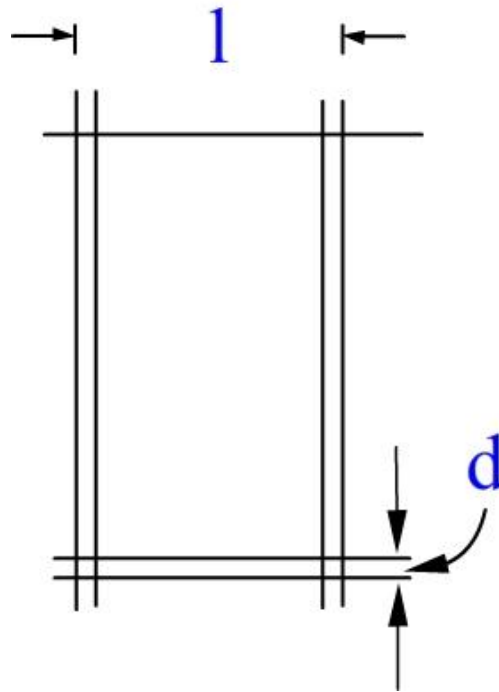


Fig.1.3 Mesh size of screens

According to Mehta and Bradshaw → If $K = 2$, turbulence is absent. According to Collar and Batchelor, if $U+u_1$ is the longitudinal velocity far upstream of the screen and $U+u_2$ the corresponding value far downstream, hence

$$\frac{u_2}{u_1} = \frac{2 - K}{2 + K}$$

so that non-uniformity is removed by a screen whose pressure drop coefficient K is equal to 2.0 and reversed if K is greater than 2.0.

1.3 Honeycombs

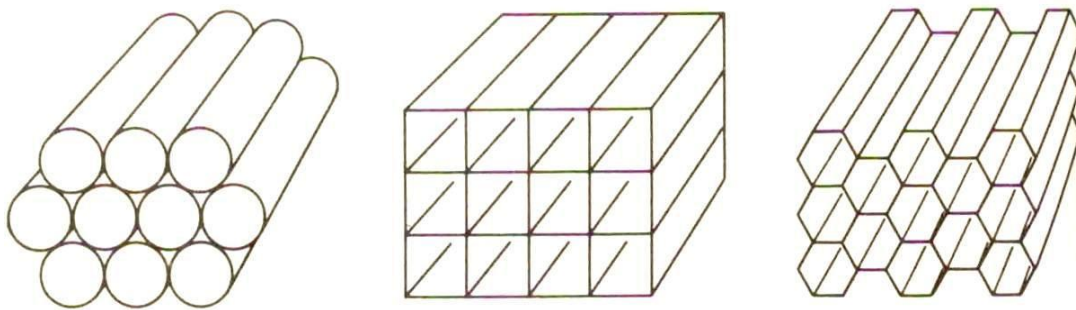


Fig.1.4 Honeycombs with different cell cross sectional shapes

Honey combs are effective in removing swirl and lateral mean fluctuations. Incidental effect is to reduce turbulence. In order to restrain the boundary layer thickness and transition in to turbulent boundary layer the cell length is usually kept within 5 to 10 times the cell dimension [Cell diameter or cell width].

1.4 Wind tunnel contractions

Wind tunnel contraction serves a few purposes

- (i) Enables velocity to be low at the location of placement of the screens.
- (ii) Reduces both mean and fluctuating velocity variations to a smaller fraction of the average velocity.
- (iii) Reduces spatial variations of velocity in the wind tunnel cross section.

The most important parameter of the contraction is the contraction ratio 'n'. The following one dimensional analysis shows how effective is the contraction in reducing the spatial non uniformity.

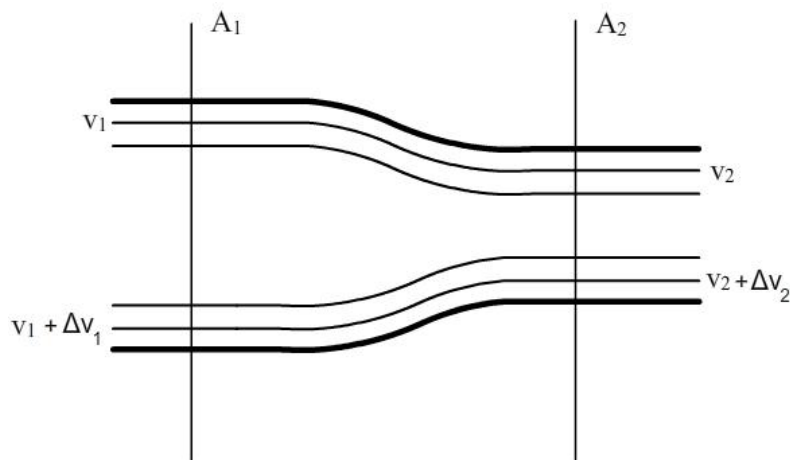


Fig.1.5 Schematic of a wind tunnel contraction

Referring to Fig.1.5 p, v and A represent present pressure, velocity and area respectively.

$a_1 = \frac{\Delta v_1}{v_1}$ is the fractional variation of velocity at the inlet to the contraction.

$a_2 = \frac{\Delta v_2}{v_2}$ is the fractional variation of velocity at the exit of the contraction $n = \frac{A_1}{A_2}$ is the contraction ratio.

$$p_1 + \frac{\rho v_1^2}{2} = p_2 + \frac{\rho v_2^2}{2}$$

$$p_1 + \frac{\rho}{2} (v_1 + \Delta v_1)^2 = p_2 + \frac{\rho}{2} (v_2 + \Delta v_2)^2$$

$$v_1 \Delta v_1 = v_2 \Delta v_2$$

$$\Delta v_1 = \Delta v_2 \frac{v_2}{v_1}$$

$$a_1 = \Delta v_2 \frac{v_2}{v_1^2} = \Delta v_2 \frac{v_2}{\left(\frac{v_2}{n}\right)^2} = n^2 a_2$$

1.5 The diffuser

The diffuser in the wind tunnel serves the purpose of salvaging the kinetic energy of flow in the test section as pressure energy. A well designed diffuser does this efficiently. In subsonic wind tunnels, the diffusers are diverging passages with a semi divergence angle of about 7.5 to 8.0 degrees. The Bernoulli's equation written in differential form in the context of a diffuser is as follows:

$$d\left(\frac{v^2}{2}\right) + \frac{dp}{\rho} = 0$$

This implies that for a decrease of kinetic energy $d\left(\frac{v^2}{2}\right)$ per unit mass, there is a corresponding increase in pressure energy. The pressure gradient in a subsonic diverging passage is adverse. It is difficult to avoid boundary layer thickening and flow separation. Hence, the conversion of kinetic energy into pressure energy is never fully efficient.

The efficiency of the diffuser is best understood in physical terms when the efficiency term is included in the Bernoulli's equation as below:

$$\eta_D \left(\frac{dv^2}{2} \right) + \frac{dp}{\rho} = 0 \quad \text{where } \eta_D \text{ is the diffuser efficiency}$$

Pressure changes in expanding passages may be examined by referring to the Fig.1.6 to elucidate the statement above.

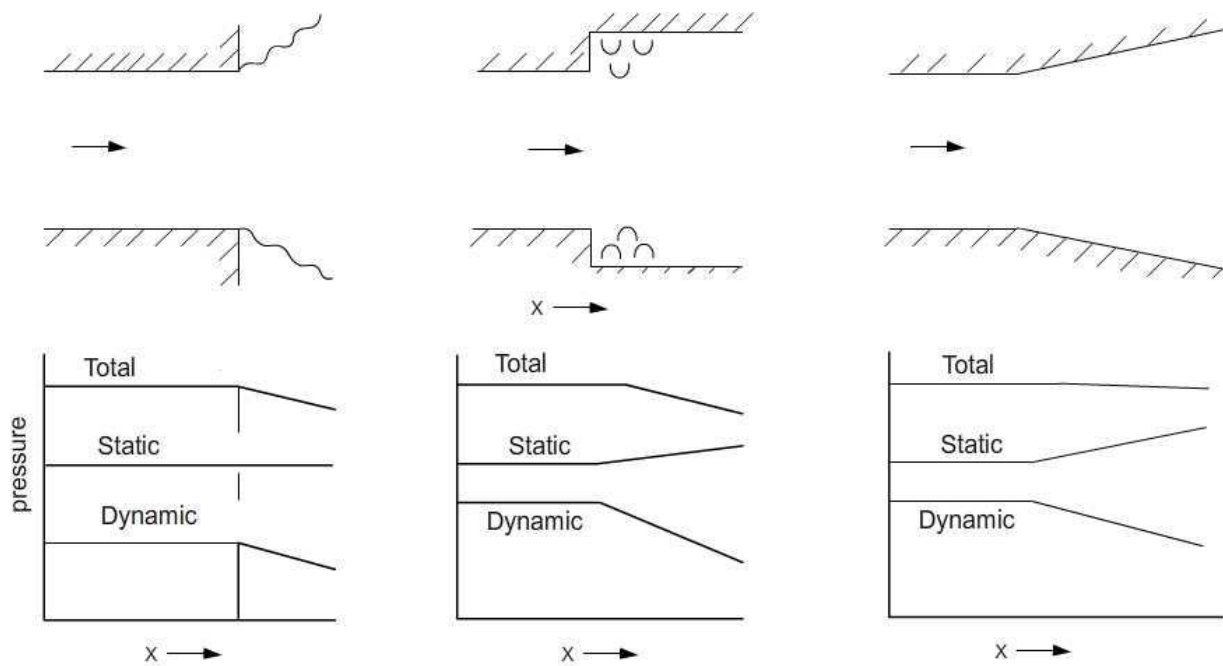


Fig.1.6 Exit pressure profile of jet through different passages

There are two definitions of diffuser efficiency

(a) Polytropic efficiency (η_D)

$$\eta_D = \frac{p_2 - p_1}{\frac{1}{2}\rho v_1^2 - \frac{1}{2}\rho v_2^2}$$

Use continuity equation to write the above equation as

$$\eta_D = \frac{p_2 - p_1}{\frac{1}{2} \rho v_1^2 \left[1 - \left(\frac{A_1}{A_2} \right)^2 \right]}$$

where subscripts '1' and '2' refer to conditions at the entry and exit of the diffuser.

As explained before, the equation is indicative that from kinetic energy to pressure energy it is not fully converted. Loss of total head in the diffuser action:

$$\Delta H = \left(\frac{1}{2} \rho v_1^2 - \frac{1}{2} \rho v_2^2 \right) - (p_2 - p_1)$$

$$\eta_D = 1 - \frac{\Delta H}{\frac{1}{2} \rho v_1^2 \left[1 - \left(\frac{A_1}{A_2} \right)^2 \right]}$$

(b) Isentropic efficiency

Isentropic Efficiency (η_σ) is defined as the ratio of

$$\eta_\sigma = \frac{\text{Kinetic energy which would have to be transformed to produce the observed pressure recovery}}{\text{Kinetic energy actually transformed}}$$

$$\left(\frac{p}{\rho^\gamma} \right) = \text{constant for an isentropic process}$$

$$\text{KE to be transformed to raise pressure from } p_1 \text{ to } p_2 = \int_{p_1}^{p_2} \frac{dp}{\rho}$$

$$\int_{p_1}^{p_2} \frac{dp}{\rho} = \frac{\gamma}{\gamma-1} \frac{p_1}{\rho_1} \left[\left(\frac{p_2}{p_1} \right)^{\frac{\gamma-1}{\gamma}} - 1 \right]$$

$$\eta_\sigma = \frac{\gamma}{\gamma-1} \frac{p_1}{\rho_1} \left[\left(\frac{p_2}{p_1} \right)^{\frac{\gamma-1}{\gamma}} - 1 \right]$$

$$\frac{p_2}{p_1} = \left[\frac{(\gamma-1)M_1^2}{2} \eta_\sigma + 1 \right]^{\gamma/\gamma-1}$$

$$\frac{p_1}{H} = \frac{p_1}{p_{01}} = \left[\frac{2}{2 + (\gamma-1)M_1^2} \right]^{\gamma/\gamma-1}$$

Overall pressure ratio $\frac{p_{01}}{p_2} = \frac{H}{p_2}$. Here p_2 corresponds to the pressure at the exit of the diffuser and H represents the stagnation pressure p_{01} at the entry to the wind tunnel.

$$\frac{H}{p_1} \times \frac{p_1}{p_2} = \left[\frac{2 + (\gamma - 1)M_1^2}{2 + (\gamma - 1)M_1^2 \eta_\sigma} \right]^{\gamma / \gamma - 1}$$

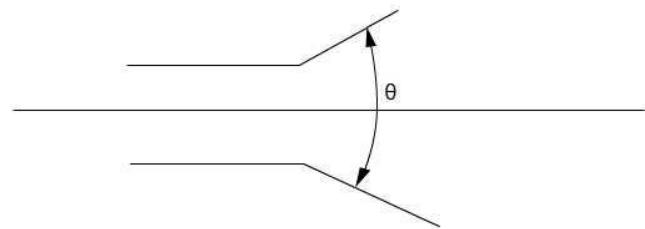
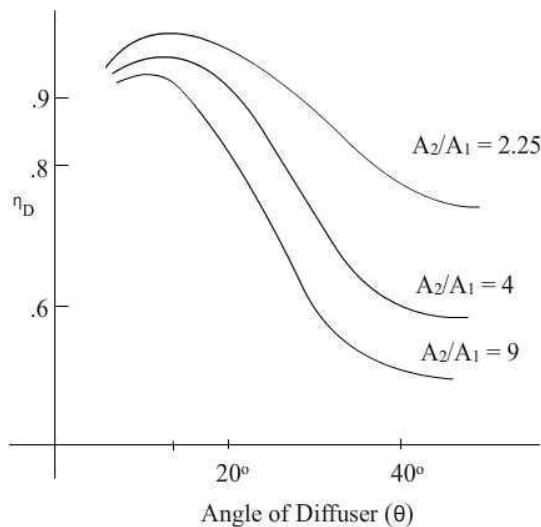


Fig.1.7 Diffuser efficiency as a function of diffuser angle

1.5 Losses in the wind tunnel circuit

Losses are due to:

- Inefficiency of drive unit
- Skin friction, separation etc
- Loss of kinetic energy at the diffuser exit
- Shocks in the case of supersonic wind -tunnels

Losses due to skin friction

$$\text{Local coefficient of skin friction} = \frac{\text{Frictional force}}{\frac{1}{2}\rho v^2 A'}$$

where, A' is the surface area of the solid boundary which is subjected to frictional force.

$$\Delta H = \int C_f \frac{1}{2} \rho v^2 \frac{L}{A} dS$$

Integral is taken over the length of the duct.

L is the perimeter, ds is an element of length in the direction of flow.

A is the cross sectional area and

C_f depends on nature of the boundary layer, Reynolds number and on the surface nature.

Losses due to resistance in the wind tunnel circuit

Corner vanes, gauzes and screen offer resistance

$$\text{Resistance Coefficient } C = \frac{\text{Resistance force}}{\frac{1}{2}\rho v^2 A} = \frac{\Delta H}{\frac{1}{2}\rho v^2}$$

$$vA = \text{constant}$$

$$v = \frac{\text{constant}}{A}$$

$$\Delta H \propto \frac{C}{A^2}, \text{ which shows that the power loss is less for large areas.}$$

1.6 Power requirements – Power economy

Power Factor is defined as

$$\lambda = \frac{\text{Power Input}}{\text{Rate of flow of kinetic energy in the test section}} = \frac{P}{\frac{1}{2}\rho v^3 A}$$

where P is the power input. Of the power P, only ηP is communicated to the air stream where η is the efficiency of the drive unit (fan efficiency).

$$\lambda = \frac{\sum \text{losses}}{\eta \frac{1}{2}\rho v^3 A} \quad \eta P = \text{losses in the wind tunnel.}$$

Reciprocal of the power factor is an alternative measure of the efficiency of the system.

Power economy

$$P = \lambda \frac{1}{2} \rho v^3 A$$

$$= \lambda \frac{1}{2} \rho v^2 v A$$

$$\text{Re} = \frac{\rho v c}{\mu}, \quad M = \frac{v}{a}$$

$$a^2 = \gamma R T = \frac{\gamma p}{\rho}$$

$$\rho = \frac{\gamma p}{a^2}$$

$$a^2 = \gamma \frac{R^*}{M} T$$

$$v = \frac{\text{Re} \mu}{\rho c}$$

substituting from above

$$P = \lambda \frac{1}{2} \frac{\text{Re}^2 \mu^2}{\rho^2 c^2} A M a \rho$$

$$= \frac{1}{2} \lambda \frac{A}{c^2} \text{Re}^2 M \frac{\mu^2 a^3}{\gamma p}$$

→ The ratio $\frac{A}{c^2}$ = the tunnel interference, is constant.

→ The power factor depends largely on the geometry of the tunnel and on the Mach and Reynolds numbers.

1.6.1 Power economy by pressurization

For tunnels of similar geometry, operating at given Re and M.

$$\rho \propto \frac{\mu^2 a^3}{\gamma p} \quad \text{Expressing in terms of stagnation properties,}$$

$$\alpha \frac{\mu_0^2 a_0^3}{\gamma p_0}$$

$$p \propto \frac{1}{p_0} \quad \text{Power is inversely proportional to } p_0.$$

Objections to power economy by pressurization

Aerodynamic forces on the model are proportional to $\frac{1}{2} \rho v^2 = \left[\frac{1}{2} \gamma p M^2 \right]$

which for given M is proportional to p_0

1.6.2 Power economy by choice of working fluid

For a given pressure $\rightarrow p \propto \frac{\mu_0^2 a_0^3}{\gamma}$

At constant temperature $a_0^3 \propto \left(\frac{\gamma}{M} \right)^{3/2}$

$$a^3 = \left(\frac{\gamma R^* T}{M} \right)^{3/2}$$

μ_0 falls as the number of atoms in a molecule increases.

$$\gamma = \frac{2n+3}{2n+1} \quad \text{where } n \text{ is the number of atoms in the molecule.}$$

γ falls when n increases.

$p \propto \frac{\mu_0^2 \gamma^{1/2}}{M^{3/2}} \rightarrow$ Power economy can be achieved by working fluid of higher molecular weight.

Limitations

\rightarrow Complete dynamic similarity can be got with only the same γ .

\rightarrow Boiling point of higher molecular weight fluids is high. Hence, to keep the working fluid in gaseous state, the temperature should be high.

Table 1.1 Power required with a different working substance

$$T_0 = 288 \text{ K}$$

Fluid	Boiling Point K			Power relative to air
Air	90			
SF ₆	222	$a_{0 \text{ SF}_6} / a_{0 \text{ Air}}$ = 0.395	$\mu_{0 \text{ SF}_6} / \mu_{0 \text{ Air}}$ = 0.529	0.020

The Table 1.1 above shows that the power required when SF₆ is used as the working fluid is only 1/50 of that while using air.

1.6.3 Power economy by reduction in stagnation temperature

For a given working fluid, p_0 , λ , M and Re .

$$P \propto \mu_0^2 a_0^3$$

$$a_0 \propto T_0^{1/2}$$

$$\mu_0 \propto \frac{T_0^{3/2}}{T_{0ref} + C} \quad C \text{ is a constant.}$$

$$P \propto \frac{T_0^{9/2}}{(T_{0ref} + C)^2}$$

Objections

- Reducing stagnation temperature brings down the flow temperature too. Boiling point is one consideration.
- Severe metallurgical problems at low temperatures.



SATHYABAMA

INSTITUTE OF SCIENCE AND TECHNOLOGY
(DEEMED TO BE UNIVERSITY)

Accredited "A" Grade by NAAC | 12B Status by UGC | Approved by AICTE

www.sathyabama.ac.in

School of Mechanical
Department of Aeronautical Engineering

UNIT – III - SAE1305 EXPERIMENTAL AERODYNAMICS

Unit 3 High speed wind tunnels

3.0 Definition of high speed

When compressibility effects are pre dominant the flow is generally said to be of high speed. A lower limit is approximately $M=0.5$. Power requirements vary as cube of velocity in the wind tunnel. This does not hold into the high speed regime exactly. Because of large power requirements, high speed wind tunnels are of the intermittent type.

3.1 Types of high speed wind tunnels

1. Continuous (for all speed ranges)
2. Intermittent

2.1 Blowdown (Fig 3.1) } $\rightarrow M > 0.5 < 5.0$

2.2 Indraft (Fig 3.2)

2.3 Intermittent pressure vacuum tunnel for $M > 5$

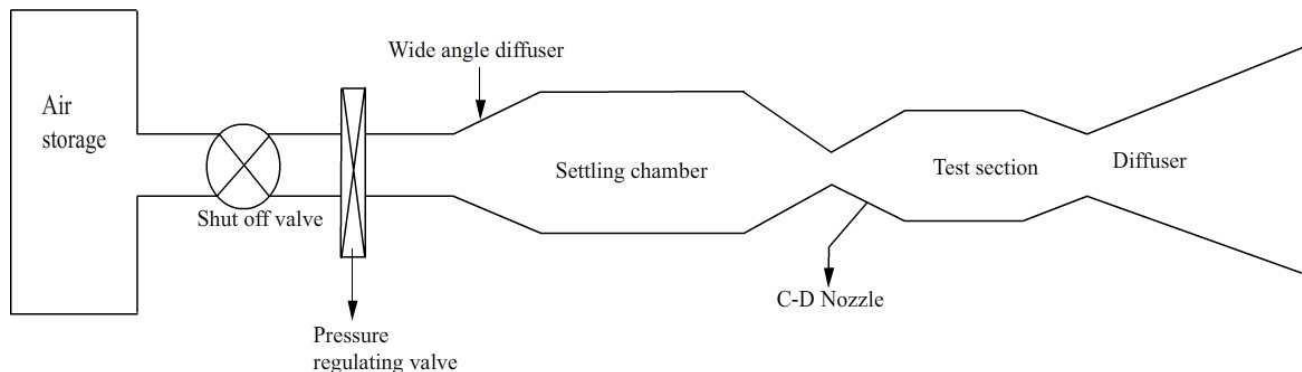


Fig.3.1 Pressure driven blow down supersonic wind tunnel

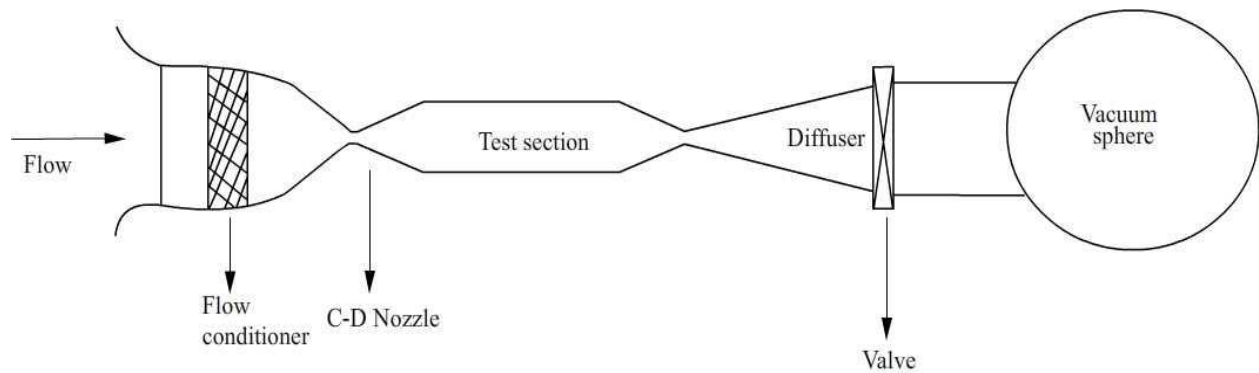


Fig 3.2 Indraft type wind tunnel

Table 3.1 Comparison between Indraft and Pressure driven wind tunnels

Indraft wind tunnels	Pressure driven wind tunnels
Stagnation temperature at supply condition is constant during a run. So also is total pressure. No fluctuations as those generated by a pressure regulator.	Reynolds number can be varied at a particular Mach no.
No possible contamination such as that due to oil.	Cost is much less than of an indraft tunnel.
Vacuum is safer to handle than pressure.	
Pressure regulators are not needed.	

The wind tunnels described above can be converted as continuous tunnels. The comparison between blow down and continuous wind tunnels are as given in Table 3.2

Table 3.2 Comparison between intermittent and continuous wind tunnels

Intermittent(blow down) wind tunnels	Continuous wind tunnels
Simple to design and less costly	More in control of conditions and return to a given test condition with more accuracy.
A single drive may run several Tunnels	Check points are easily obtained No panic of rapid testing
Model testing is more convenient	Test conditions can be held constant for a longer time.
Extra power is available to start	
Failure of model will not result in tunnel damage	

3.2 Supersonic wind tunnels

Introduction

The nozzle regulates the speed of air entering the test section (T.S) of the wind tunnel so that the desired Mach number is established. Mach number is uniquely determined by the area ratio of the nozzle. A well designed nozzle makes the flow parameters uniform across the cross section. The design of a suitably shaped nozzle contour to obtain the desired uniform flow at the nozzle exit is based on the method of characteristics.

3.2.1 Test section parameters

(i) Dynamic pressure

The local dynamic parameter $\frac{1}{2}\rho v^2$ can be related to the local Mach number and static pressure.

$$q = \frac{1}{2} \rho v^2 = \frac{1}{2} \frac{p}{RT} v^2$$

$$= \frac{1}{2} \frac{p}{\gamma RT} \gamma v^2 = \frac{1}{2} \gamma p M^2$$

(ii) Mass flow rate

$$\dot{m} = \rho v A = \rho^* a^* A^*$$

* represents choked conditions ($M = 1$)

$$\frac{\dot{m}}{A} = \frac{\rho A v}{A^*} \cdot \frac{A^*}{A}$$

$$= \frac{\rho^* A^* v^*}{A^*} \frac{A^*}{A}$$

Since, $\rho^* = \frac{p^*}{RT^*}$ and $v^* = a^* = \sqrt{\gamma RT^*}$

One has

$$\frac{\dot{m}}{A} = \frac{p^*}{RT^*} \sqrt{\gamma RT^*} \frac{A^*}{A}$$

$$= \sqrt{\frac{\gamma}{R}} \frac{p^*}{\sqrt{T^*}} \frac{A^*}{A}$$

Using equation for $\frac{T^*}{T_0}$ and $\frac{p^*}{p_0}$

and writing in terms of stagnation conditions,

$$\frac{T_0}{T} = 1 + \frac{\gamma-1}{2} M^2$$

$$\frac{T_0}{T^*} = 1 + \frac{\gamma-1}{2} = \frac{2+\gamma-1}{2} = \frac{\gamma+1}{2}$$

When $M = 1$,

$$\frac{p_0}{p^*} = \left(\frac{\gamma+1}{2} \right)^{\frac{\gamma}{\gamma-1}}$$

$$\frac{\dot{m}}{A} = \sqrt{\frac{\gamma}{R}} \frac{p_0}{\sqrt{T_0}} \frac{\left(\frac{2}{\gamma+1}\right)^{\frac{\gamma}{\gamma-1}}}{\left(\frac{2}{\gamma-1}\right)^{1/2}} \frac{A^*}{A}$$

$$\frac{\dot{m}}{A} = \sqrt{\frac{\gamma}{R}} \frac{p_0}{\sqrt{T_0}} \left(\frac{2}{\gamma+1}\right)^{\frac{\gamma+1}{2(\gamma-1)}} \frac{A^*}{A}$$

Mass flow density is expressed as a function of stagnation conditions and the area ratio.

For isentropic flow, A^* is a constant and $\frac{A}{A^*}$ is a unique function of local Mach number.

$$\frac{A}{A^*} = \frac{1}{M_1} \left(\frac{1 + \frac{\gamma-1}{2} M^2}{\frac{\gamma+1}{2}} \right)^{\gamma+1/2(\gamma-1)}$$

$$\frac{\dot{m}}{A} = \sqrt{\frac{\gamma}{R}} \frac{p_0}{\sqrt{T_0}} M \left(1 + \frac{\gamma-1}{2} M^2 \right)^{-\frac{\gamma+1}{2(\gamma-1)}}$$

(iii) Test section velocity

$$V = a M$$

$$= \left(\frac{\gamma R T_0 M^2}{1 + \frac{\gamma-1}{2} M^2} \right)^{\frac{1}{2}}$$

(iv) Maximum velocity

$$c_p T + \frac{v^2}{2} = c_p T_0$$

v is maximum when $c_p T = 0$

$$c_p - c_v = R$$

$$c_p / c_v = \gamma$$

$$c_p - \frac{c_p}{\gamma} = R$$

$$\frac{c_p \gamma - c_p}{\gamma} = R$$

$$\frac{c_p (\gamma - 1)}{\gamma} = R$$

$$c_p = \frac{\gamma R}{\gamma - 1}$$

$$v_{\max}^2 = 2c_p T_0$$

$$v_{\max} = \left(\frac{2\gamma R}{\gamma - 1} T_0 \right)^{\frac{1}{2}}$$

The test section flow velocity v for a given stagnation temperature T_0 approaches the maximum value v_{\max} at relatively low supersonic Mach numbers.

For example,

In the case of $T_0 = 300\text{K}$

$$R = 287\text{J/kgK}$$

and a test section Mach number of 5.0, the ratio of v/v_{\max} can be calculated to see that it is equal to 0.913. This means at ordinary stagnation temperatures, the velocity in the test section reaches 91% of the maximum possible velocity corresponding to the total energy of the fluid. The stagnation temperature T_0 rather than the Mach number which is important to attain high velocities.

(v) Free stream Reynolds Number (Re)

$$\text{Re} = \frac{\rho v L}{\mu}$$

Experimental observation is that μ is independent of pressure in the range of 0.001 to 20 atmospheres.

$$\left(\frac{\mu}{\mu_0}\right) = \left(\frac{T}{T_0}\right)^n \text{ for air } n = 0.768$$

$$\frac{\mu}{\mu_0} = \frac{T_0 + C}{T + C} \left(\frac{T}{T_0}\right)$$

$$C = 130$$

$$\frac{\rho}{\rho_0} = \left(\frac{T}{T_0}\right)^{\frac{1}{\gamma-1}}$$

If this relation is assumed then the free stream Re can be expressed as a function of M_1 , the T.S Mach no and of the stagnation parameters. Reynolds no per unit length $\frac{Re}{L} = \frac{\rho v}{\mu} \rightarrow \rho, v, \mu$ are expressed in stagnation quantities as given below.

$$\frac{\rho}{\rho_0} = \left[1 + \frac{\gamma-1}{2} M^2\right]^{-\frac{1}{\gamma-1}}$$

$$\rho = \rho_0 \left[1 + \frac{\gamma-1}{2} M^2\right]^{-\frac{1}{\gamma-1}}$$

$$\mu = \mu_0 \left(\frac{T}{T_0}\right)^n = \mu_0 \left(\frac{1}{1 + \frac{\gamma-1}{2} M^2}\right)^n$$

$$M = \frac{v}{a}$$

$$v = Ma$$

$$= Ma \left(\frac{1}{1 + \frac{\gamma-1}{2} M^2}\right)^{\frac{1}{2}}$$

$$\frac{a^2}{a_0^2} = \frac{\gamma RT}{\gamma RT_0}$$

$$\frac{Re}{L} = \frac{\rho_0 \left[1 + \frac{\gamma-1}{2} M^2 \right]^{-\frac{1}{\gamma-1}}}{\mu_0 \left[\frac{1}{1 + \frac{\gamma-1}{2} M^2} \right]^n} * M a_0 \left(\frac{1}{1 + \frac{\gamma-1}{2} M^2} \right)^{\frac{1}{2}}$$

n= 0.768 for air

Simplifying

$$\frac{Re}{L} = \frac{\rho_0}{\mu_0} a_0 M \left[1 + \frac{\gamma-1}{2} M^2 \right]^{0.268 - \frac{1}{\gamma-1}}$$

Both a_0 and μ are functions of stagnation temperature. Both increase with temperature. Hence, appreciable changes in free stream Re/unit length for a given M can be obtained only by varying stagnation density.

3.3 Components of supersonic wind tunnels

3.3.1 Air storage tanks

Size of the storage will be dependent on the mass flows required and the frequency of runs. Pressure storage tanks are available on the shelf basis – They are mounted horizontally or vertically. Tanks are painted black to absorb heat. They are provided with safety disk or pressure relief valve. As air is drawn from the storage, polytropic expansion takes place within the tank. This results in drop of reservoir temperature which is very bothersome. Fall of stagnation temperature causes resultant change in the stream temperature for a given Mach

number. Change in temperature results in the change of viscosity which in turn affects the boundary layer thickness. Changes in Reynolds number and Mach number during a run are thus consequential to the fall in reservoir temperature.

To maintain constancy of stagnation temperature, it is a practice to stack the reservoir volume with empty metallic cans. They serve as heat storing matrix during compression and release heat during the expansion process. Another way to maintain the constant stagnation temperature is by providing heater units in the reservoir.

3.3.2 Settling chamber /wide angle diffusers

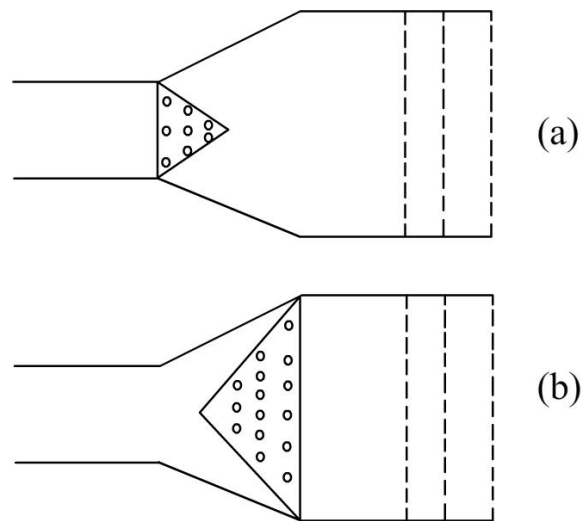


Fig.3.3a, b Wide angle diffuser

Wide angle diffusers lead the flow to the settling chamber. Arrangements for leading the flow to the settling chamber may be by one of the methods shown in Figure 2.3a, b or c.

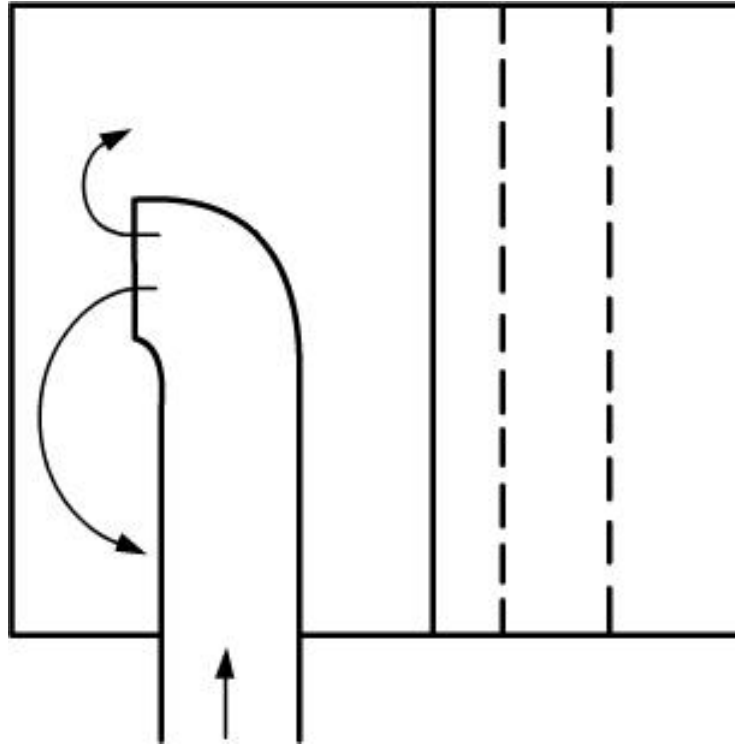


Fig.3.3c Reverse entry into the settling chamber

Uniformity of flow in the test section is improved if a large area ratio contraction is provided.

3.3.4 Convergent-divergent (c-d) nozzle

The c-d nozzle forms the heart of the supersonic wind tunnel .For generating supersonic flow in the test section, it is essential that there is a c-d nozzle in the tunnel circuit before the test section. The area ratio of the c-d nozzle ($A_{\text{exit}}/A_{\text{throat}}$) uniquely decides the Mach number.

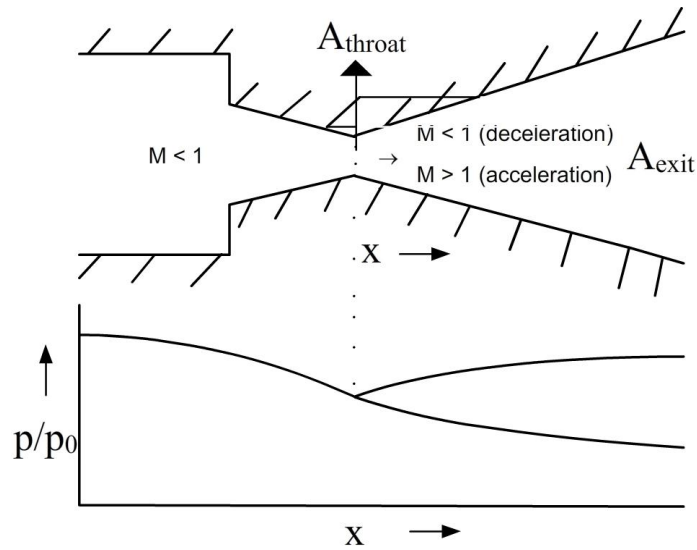


Fig.3.4 Convergent divergent nozzle and the pressure profile

When the tunnel operation starts, the flow is initiated in the nozzle as subsonic and reaches the sonic Mach number at the throat when sufficient mass flow is allowed. This is called the choked condition of the nozzle. Under this condition, maximum mass flow rate for the given stagnation conditions takes place through the nozzle. The ratio between the upstream stagnation pressure (P_0) and the downstream back pressure (P_b) corresponding to the first time choking is called the first critical pressure ratio of the nozzle. At this pressure ratio, the flow in the divergent part of the nozzle is subsonic. The exit Mach number will be the subsonic value corresponding to the A/A^* in the Fig.2.5. In this context A is the exit area and A^* the throat area of the choked nozzle. As the value of P_0/P_b is progressively increased, the flow in the divergent part of the nozzle accelerates to be supersonic but shocks are formed in the divergent part until a pressure ratio corresponding to the supersonic Mach number of the nozzle is reached. The pressure ratio corresponding to this Mach number is the third critical pressure ratio of the nozzle. Between the first and third critical pressure ratios shocks of varying strengths take place in the nozzle and outside of it as there is no other isentropic solution between the 1st and 3rd critical pressure ratios. The pressure ratio corresponding to the occurrence of a shock at the exit plane of the nozzle is the second critical pressure ratio of the nozzle.

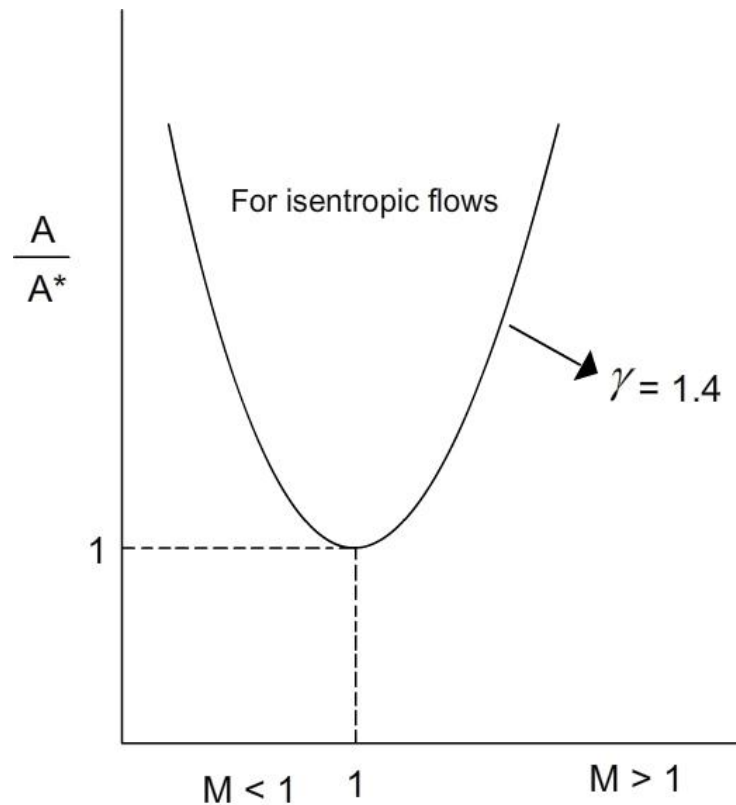


Fig.3.5 A/A* vs. Mach numbers

All the shocks generated at the different pressure ratios inside the nozzle will make the post shock Mach number subsonic and the subsonic nozzle exit pressure will be made equal to the ambient pressure in the remaining part of the diffusing divergent channel. Between the second and third critical pressure ratios, oblique shocks of varying strengths depending on the pressure ratio will be formed emanating from the nozzle lip. The physical purpose of these oblique shocks is equalization of pressures between the exit plane and the ambient. If the pressure ratio is increased beyond that corresponding to the third critical pressure ratio, expansion fans will be formed at the lip of the nozzle.

3.3.5 Diffuser- the necessity of providing a diffuser

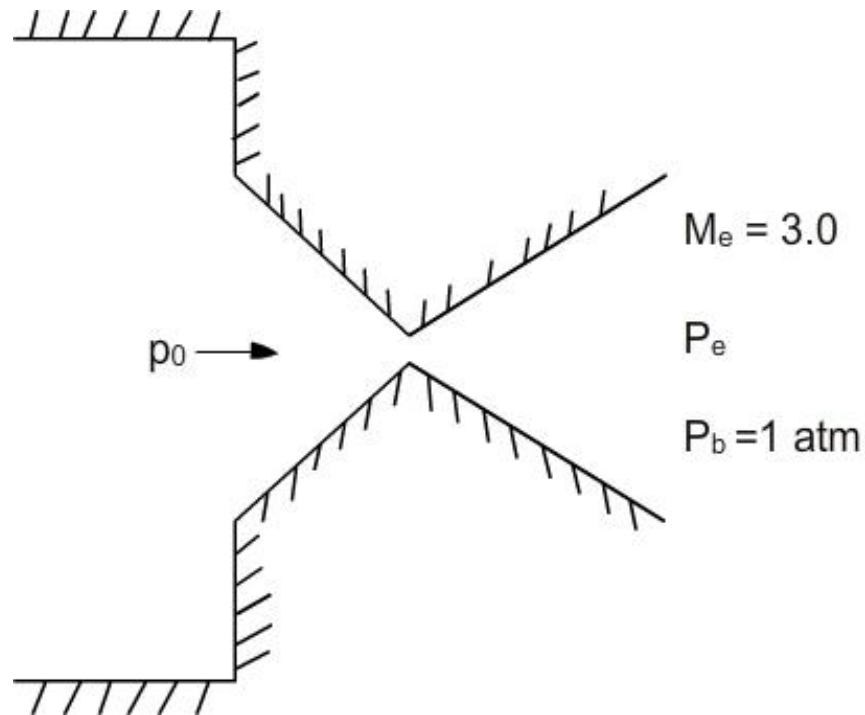


Fig.2.6 a Nozzle of a free jet facility

Take the case of a free jet facility as in Fig.3.6 making use of a c-d nozzle of Mach number 3.0 exiting to the ambient conditions at one atmosphere pressure. In order to avoid shocks and expansion waves at the exit of the nozzle, p_e must be p_b .

$$\left(\frac{p_o}{p_e} \right)_{M=3} = 36.7$$

Pressure ratio required will be $\frac{p_o}{p_e} = 36.7$ for a wave free exit flow from the nozzle.

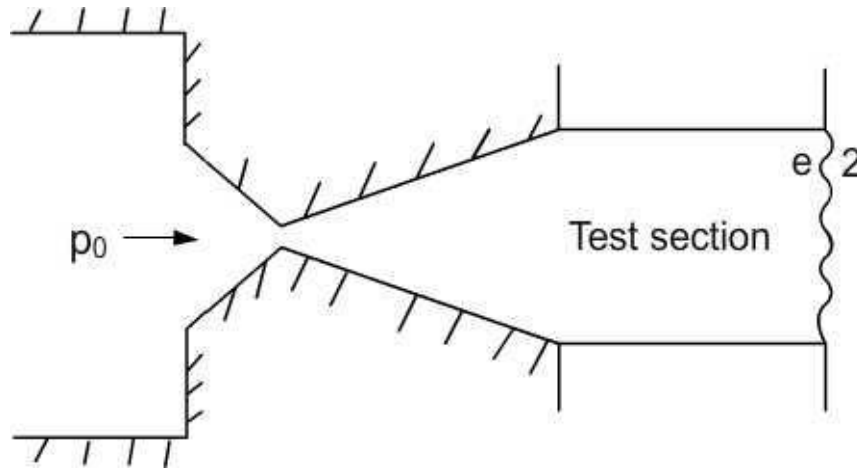


Fig.3.6 b Free jet nozzle with a test section

In the Figure 3.6b, a constant area section is added to the nozzle exit. The duct similar to the test section (T.S) of a wind tunnel attached to the nozzle exhausts to atmosphere. p_e corresponds to static pressure at the exit plane of the nozzle before the shock. Static pressure after the shock (p_2) is equal to ambient pressure.

$$\frac{p_o}{p_2} = \left(\frac{p_o}{p_e}\right) \times \left(\frac{p_e}{p_2}\right) = 36.7 \times \left(\frac{1}{10.33}\right) = 3.55$$

In the equation above, p_e/p_2 represents the shock pressure ratio at $M=3.0$.

In the third case, as in Figure 2.8 a divergent channel is provided after the constant area duct and the shock stands at the end of the constant area duct.

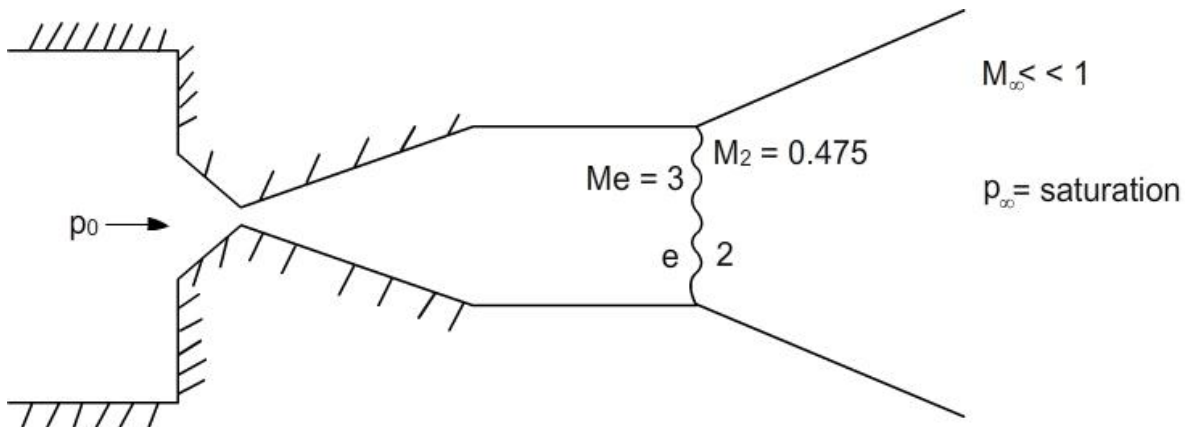


Fig.3.8 Free jet facility with test section and a diffuser

When $M \ll 1$, $p_o = p_\infty$

$$\frac{p_o}{p_\infty} = \left(\frac{p_0}{p_e} \right) \left(\frac{p_e}{p_2} \right) \left(\frac{p_2}{p_{o2} = p_\infty} \right)_{M=0.475} = 36.7 \times \frac{1}{10.33} \times 0.856 = 3.04$$

The three cases described above make it clear that provision of a diffuser of suitable design is required for reducing the pressure ratio required for the operation of the wind tunnel. It is shown in section 2.5 that the power required to run the wind tunnel increases with the pressure ratio. In supersonic wind tunnels, most commonly used diffuser is of convergent divergent type (also called the second throat diffuser).

3. 4 Power required for the operation of supersonic wind tunnel

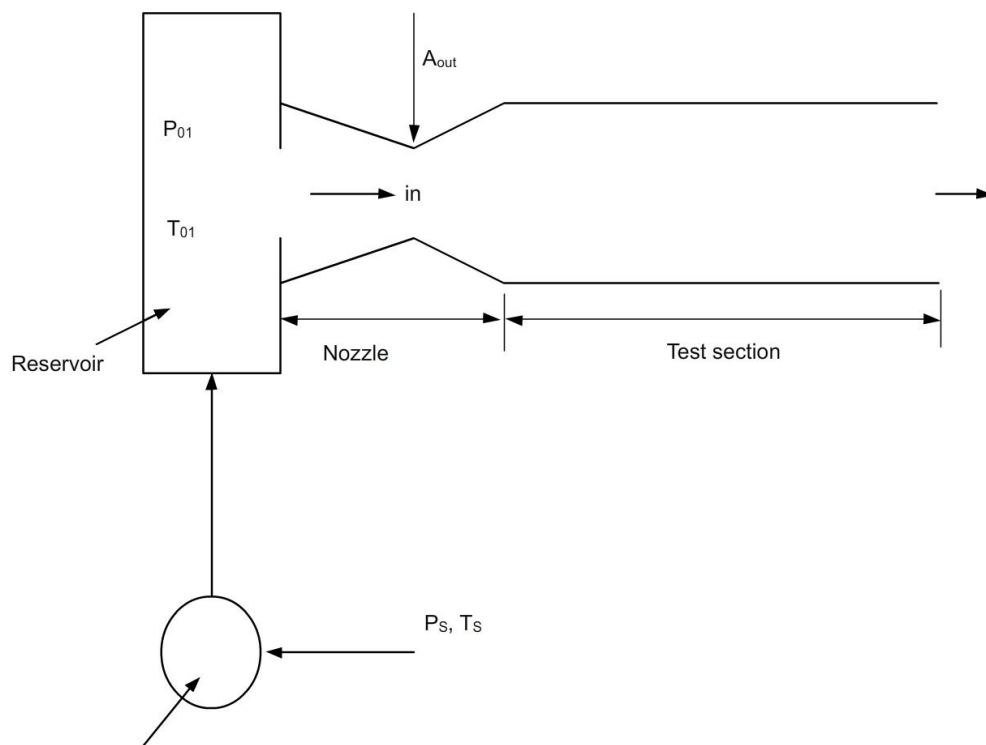


Fig.3.9 Free jet type wind tunnel with an attached test section

Refer to figure 2.7 where a free jet type wind tunnel is shown. Let the supersonic tunnel is specified by the Mach number (M) in the test section and test section (A) area .The throat area

is specified as A_{NT} . The flow parameters in the test section are denoted as p , T , A etc.. Once M is specified, the area ratio A_T/A_{NT} and ratios of pressure and temperature p/p_{01} and T/T_{01} are all known from the isentropic equations. If the compressor is idealized (isentropic) the suction and reservoir conditions are related.

$$\frac{T_s}{T_{01}} = \left(\frac{p_s}{p_{01}} \right)^{\gamma-1/\gamma}$$

Where p_s and T_s represent pressure and temperature at the compressor suction. If the nozzle is choked, the mass flow rate can be written as,

$$\dot{m} = A_{NT} \sqrt{\frac{\gamma}{R}} \left(\frac{2}{\gamma+1} \right)^{(\gamma+1)/2(\gamma-1)} \frac{p_{01}}{\sqrt{T_0}}$$

The power required to operate the compressor may be found as follows:

If the compressor is isentropic, the work per unit time may be found from the enthalpy difference across the compressor.

$$\begin{aligned} \dot{W} &= -\dot{m}(h_{01} - h_s) \\ &= -\dot{m} \frac{\gamma R}{\gamma-1} (T_{01} - T_s) \quad [\dot{W} = \text{work / unit time in W or } \frac{\text{Nm}}{\text{S}}] \\ &= \frac{\dot{m} \gamma R T_s}{\gamma-1} \left(\frac{T_{01}}{T_s} - 1 \right) \\ &= -\dot{m} \gamma \frac{R T_s}{\gamma-1} \left[\left(\frac{p_{01}}{p_s} \right)^{\frac{\gamma-1}{\gamma}} - 1 \right] \end{aligned}$$

$$\dot{W} = -\dot{m} \frac{\gamma R T_s}{\gamma-1} \left[(r_p)^{(\gamma-1)/\gamma} - 1 \right]$$

The pressure ratio $\frac{p_{01}}{p_s}$ is known as the operating pressure ratio and is denoted by r_p

The very large power required for the operation of a supersonic wind tunnel is attributed to the large operating pressure ratio. If the wind tunnel is equipped with a suitably designed diffuser and a closed circuit arrangement as shown in the next section, the stagnation pressure of the diffused high velocity air can be made use of by the compressor and the effective pressure ratio can be reduced.

3.5 Closed circuit supersonic wind tunnel

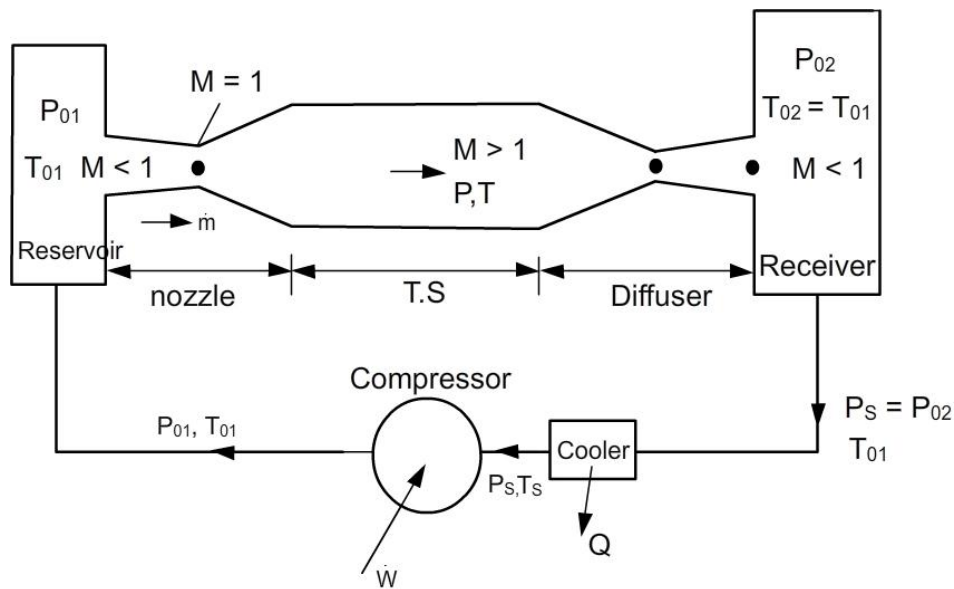


Fig.3.10 Continuous type supersonic wind tunnel

A convergent-divergent (c-d) diffuser is provided as shown in Fig.2.10. Only if the flow is isentropic, the stagnation pressure regained in the receiver following the diffuser (p_{02}) is equal to that of the flow entering the nozzle (p_{01}).

In that case, $p_{02} = p_{01}$

Then, $r_p = 1$, so that compressor does no work. In practical cases, because of entropy changes $p_{02} < p_{01}$ and $r_p > 1$. If the entropy change is confined to the region between the two throats, the diffuser throat area A_{DT} must be larger than the nozzle throat area A_{NT} . Diffuser throat area must be large enough to accommodate the stagnation pressure loss of the strongest shock. A cooler is included prior to the compressor because compressor work is proportional to the intake temperature.

The practical operation of the closed circuit wind tunnel may be explained as follows: As the tunnel is started, flow through it begins as subsonic and as the pressure ratio is increased the nozzle is choked. Further increase in the pressure ratio causes shock to be formed in the divergent section. At a pressure ratio corresponding to second critical pressure ratio, shock is formed at the exit plane of the nozzle which is same as the entry section to the test section. The formation of shocks during the starting process gives rise to fall in stagnation pressure. The total pressure after the shock is designated as p_{02} . This necessitates that the diffuser throat is designed larger as decided by the ratio p_{02}/p_{01} . The ratio of diffuser throat area to the nozzle throat is in the inverse ratio of total pressures given above.

$$\frac{A_{NT}}{A_{DT}} = \frac{p_{02}}{p_{01}} < 1$$

The ratio of areas for different test section Mach numbers calculated based on normal shock losses is given in Fig.2.11. This makes sure that the starting shock passes through the diffuser throat. The diffuser throat area calculated as above does not take in to account the non-isentropy of frictional flows and only the shock losses are considered.

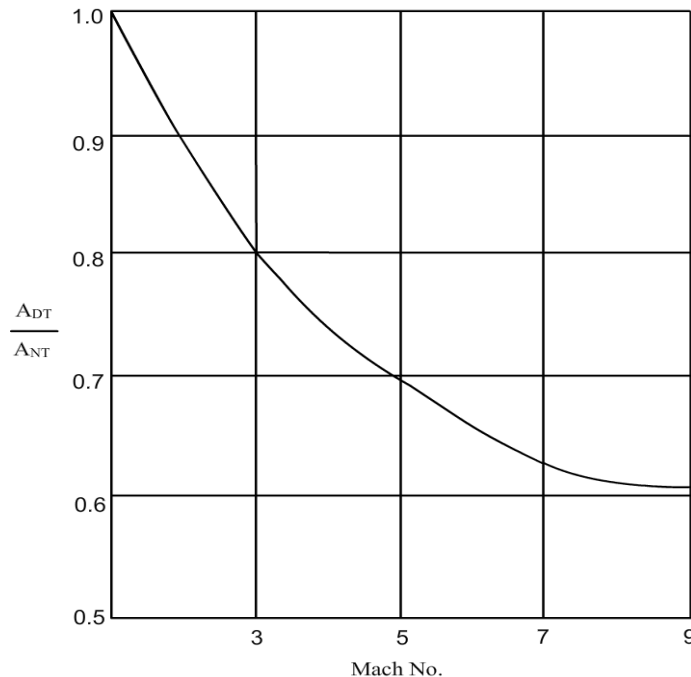


Fig.3.11 Ratio of diffuser throat and nozzle throat for different test section Mach numbers

Assuming a frictionless operation, the shock may assume any section in the constant area test section. But, the effect of friction is to make the shock unstable in the constant area duct. The shock that is generated during starting of the tunnel does not stay at the nozzle exit (entry to test section) but is moved downstream by the effect of friction.

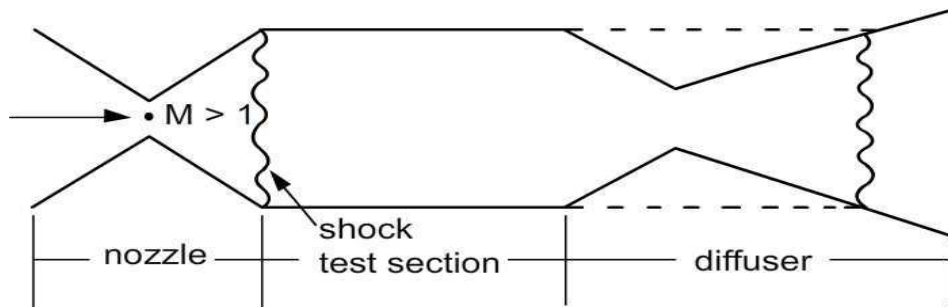


Fig.3.12 Shock movement from nozzle exit to diffuser

The starting pressure ratio minimum required to cater to the shock at the test section Mach number is corresponding to that for locating the shock at the nozzle exit. (worst shock)

$$r_{ps} = \left(\frac{p_{01}}{p_{02}} \right)_{\text{worst shock}}$$

As the starting pressure ratio is maintained, the starting shock which moves down stream can be stable only at an area equal to that of the test section. In the convergent part of the diffuser the Mach number will be less than that in the test section. With the value of starting pressure ratio which produced the shock at the test section Mach number being maintained, shock losses at that Mach number is being catered to. Hence the starting shock stabilizes only in the diverging part of the diffuser at a section where there is equal area and Mach number as the test section. The starting shock crossing the diffuser throat and remaining in its divergent part is called the ‘**swallowing of the starting shock**’.

It has to be remembered that as the diffuser throat is larger than the nozzle throat, the Mach number there will be more than one but less than that in the test section. After the brief

duration of starting, the pressure ratio may be decreased and the shock may be brought to the diffuser throat. Therefore the higher pressure ratio is required only during the starting when a shock at the test section Mach number is necessarily to be catered to and thereafter the pressure ratio can be that corresponding to shock at the diffuser throat. The smallest pressure ratio at which the tunnel may be continuously operated (r_{PO}) after its starting is that corresponding to the stagnation pressure loss of the weakest starting shock which can be made to occur at the diffuser throat.

$$r_{PO} = \left(\frac{p_{01}}{p_{02}} \right)_{\text{Shock at } M_{DT}}$$

In summary, the pressure ratio for starting the wind tunnel is corresponding to the normal shock losses at the test section Mach number and that for operation is that corresponding to normal shock losses at the diffuser throat. Hence the power required can be considerably reduced by incorporating the well designed diffuser and by judicious control of the two pressure ratios during ‘starting’ and ‘operating’ of the wind tunnel.

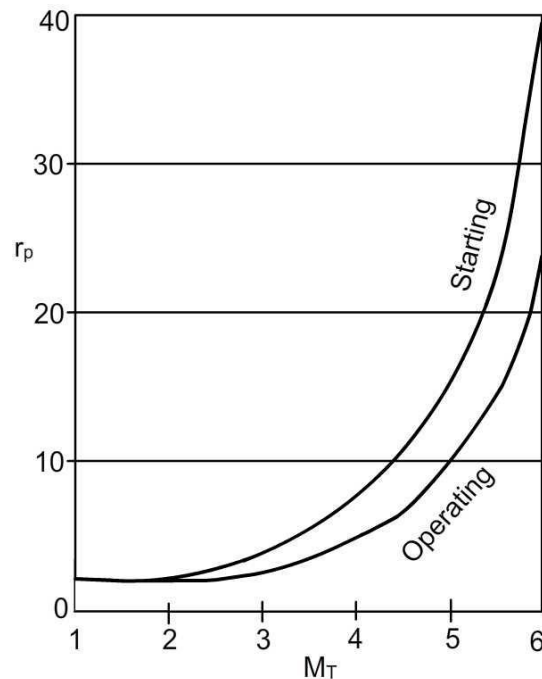


Fig.3.11 Pressure ratios for starting and operating the wind tunnel of different Mach numbers

3.6 Actual flow in the supersonic wind tunnel

The boundary layer (B.L) thickness and the total loss of momentum increase with increasing distance from the 1st throat. The growth of boundary layer thickness with distance from first throat is predictable and can be accounted for in the nozzle design. In the steady state operation, viscous effects between the throat and test section are not of much importance.

During the transient process in which tunnel is started, viscous effects are much important. So, important are these effects that pressure ratios required to start high Mach number tunnels are atleast 100% greater than the normal shock pressure ratio $\frac{p_{01}}{p_{02}}$ i.e. viscous losses are almost equal to normal shock losses.

B.L. is stable when the pressure is decreasing in the direction of its growth. When the pressure is increasing in the direction of flow, it has a tendency to separate. As normal shock passes through the nozzle, it imposes a severe unfavorable pressure gradient which can cause separation. If B.L separates, it disturbs the flow over a large portion of nozzle. If B.L. does not separate the high pressure gain in the downstream of shock will tend to flow to low pressure B.L. and the flow in the duct will be altered over a significant length of the nozzle. In the diffuser viscous effects are predominant during starting and steady state operation of the wind tunnel. Unfavorable pressure gradient exists always. An oblique shock from the convergence creates additional pressure gradients when they strike the opposite wall.

3.6.1 Starting a tunnel with a model in the test section

It is explained earlier that

$$\frac{A_{DT}}{A_{NT}} = \frac{p_{01}}{p_{02}}$$

which implies that losses in total head resulting from shocks necessitate a larger diffuser throat. Hence, losses due to shocks on the model must also be provided for. So, for starting a tunnel with a model, a second throat larger than that for a clear tunnel is needed.

3.6.2 Sizing the wind tunnel model

The theoretical unobstructed cross section area of the test section at the model required for starting is the same as the second throat area.

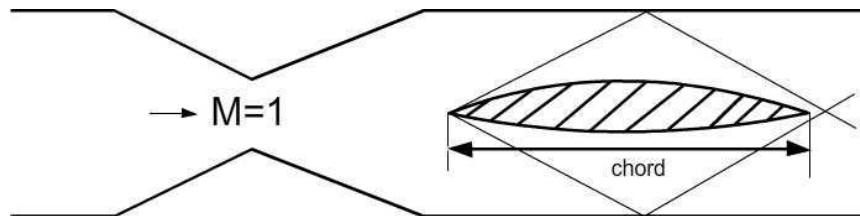


Fig.3.12 Typical shock wave pattern from a model

In choosing the dimensions of the model, reflection of shocks should be also considered. The oblique shocks formed as shown in Figure 2.12 at the leading edge of the model get reflected from the wind tunnel wall. It has to be remembered that shock reflection is not specular which means that the angle of incidence of the shock at the test section wall is not same as that for reflection. The chord length of the model is so chosen that the reflected shocks do not interfere with the model.

3.6.3 Two problems in the operation of supersonic wind tunnels

(i) Condensation

The amount of moisture that can be held by a unit volume of air increases with increasing temperature. When the air isentropically expands to higher Mach numbers in the test section, the temperature falls. It may become super cooled. Moisture will then condense.

Factors affecting condensation

- a) Amount of moisture in the stream
- b) Static temperature of the stream
- c) Static pressure of the stream
- d) Time during which the stream is at low temperature

Effects of condensation

Condensation results in changes of local Mach number and other flow properties due to latent heat addition. The extent of changes depends on how much heat is released through condensation and may be evaluated using the two equations given below:

$$\frac{dM^2}{M^2} = \frac{1 + \gamma M^2}{(\gamma - M^2)} \left[\frac{dQ}{H} - \frac{dA}{A} \right]$$

$$\frac{dp}{p} = -\frac{\gamma M^2}{1 - M^2} \left[\frac{dQ}{H} - \frac{dA}{A} \right]$$

The notations used in the equations are:

dQ = heat added through condensation

H = enthalpy per unit mass

A = duct area

When $M > 1$, Mach no decreases and pressure increases.

When $M < 1$, Mach no increases and pressure decreases.

Drying the working fluid is the best way to avoid condensation. Increasing the temperature by providing stagnation heaters is another solution.

(ii) Liquefaction

In a manner parallel to condensation, the components of air liquefy when proper temperature and pressure conditions are met. Liquefaction troubles might start around $M=4$ if high pressure air is expanded from room temperature.

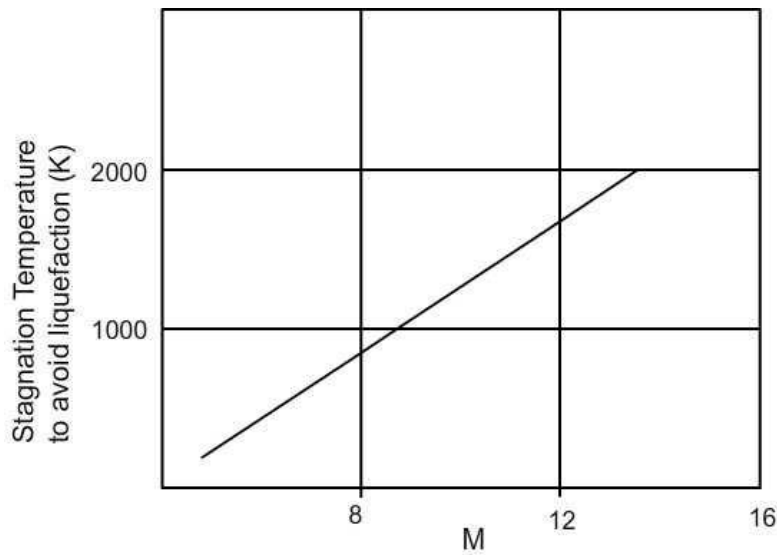


Fig.3.13 Stagnation temperature to avoid liquefaction at different Mach numbers

Fig.3.13 shows the stagnation temperature required to avoid liquefaction at different Mach numbers. It can be seen that corresponding to a Mach number above 12 the temperature required will be about 2000K.



SATHYABAMA

INSTITUTE OF SCIENCE AND TECHNOLOGY
(DEEMED TO BE UNIVERSITY)

Accredited "A" Grade by NAAC | 12B Status by UGC | Approved by AICTE

www.sathyabama.ac.in

School of Mechanical
Department of Aeronautical Engineering

UNIT – IV - SAE1305 EXPERIMENTAL AERODYNAMICS

4.1 Introduction

The visualisation of complex flows has played a uniquely important role in the improvement of our understanding of fluid dynamic phenomena. Flow visualisation has been used to verify existing physical principles and has led to the discovery of numerous flow phenomena. In addition to obtaining qualitative global pictures of the flow the possibility of acquiring quantitative measurements without introducing probes that invariably disturb the flow has provided the necessary incentive for development of a large number of visualisation techniques. The methods usually depend either on

- (i) the reflection or scattering of light by small solid or liquid particles introduced into the stream or
- (ii) on the natural changes of refractive index which accompany the density changes of a compressible fluid.

4.2 Flow visualisation by direct injection (Tracer Methods)

In this group of methods, small particles of solid or liquid are introduced into the fluid stream and observed by reflected or scattered light. It is necessary that such particles are of sufficiently small inertia to follow the local direction of fluid motion and sufficiently light as not to be sensibly influenced by gravity. Smoke or other particles in air and dye or other particles in water provide the necessary contamination for flow visualisation. Many substances have been used to visualise the flow of air and water. Smoke, helium bubbles, dust particles and even glowing iron particles have been used in air. A variety of dyes, particles, neutrally buoyant spheres and both air and helium bubbles have been employed in water.

Smokes consist of suspension of small solid or liquid particles in a transparent gas and are usually observed by the scattering and reflection of light by these particles. The word “smoke” used in flow visualisation includes a variety of smoke like materials such as vapours, fumes and mists.

A large number of materials have been used to generate smoke eg, the combustion of tobacco, rotten wood and straw the products of reaction of various chemical substances such as titanium tetrachloride and water vapour. The smokelike materials are referred to as aerosols (since aerosols are composed of collided particles suspended in a gas).

Two very practical points must be examined before the choice of smokelike material. The particles must be as small as possible so that they will closely follow the flow pattern being studied. The particles must be large enough to scatter a sufficient amount of light. Sizes below $1\ \mu\text{m}$ but above $0.15\ \mu\text{m}$ are good for scattering sufficient light and hence for photographing.

The most popular agent for airflow visualisation in wind tunnels has been smoke. The use of smoke requires a low turbulence level to minimize diffusion. Furthermore the smoke particles are so small that they cannot be observed or photographed individually. A larger neutrally buoyant tracer agent is needed to follow the paths of individual particles and bubble methods are useful in this regard.

The soap bubble is an ideal particle because its size and buoyancy can be controlled. The system for bubble method consists of a bubble generator, lighting and optical components and photographic equipments to record the paths of bubbles. Neutral buoyancy is achieved by filling the bubbles with helium. Bubbles from approximately 1 to 5mm dia can be generated at rates upto 500/sec.

4.3 Index of refraction methods

The three methods included in this category are Schlieren, Shadowgraph and Interferometric techniques. Although all three methods depend on variation of index of refraction in a transparent medium and the resulting effects on a light beam passing through the test region quite different quantities are measured with each one. All three methods are used to study density fields in transparent media.

Density is a variable in compressible fluid. Particles added in incompressible fluids for visualising flows cannot respond to the thermodynamic changes. Hence, refractive index based methods are used for visualisation of such flows.

These methods are integral. They integrate the quantity measured over the length of the light beam. So, they are suited for two dimensional flow fields where there are no density variation in the field along the light beam except at entrance and exit of test section.

4.3.1 Theoretical background

According to Gladstone – Dale formula

$$n-1 = K\rho$$

where, n is the refractive index.

K values are (to a large extent).

constant for a wavelength. Varies slightly with λ .

Table 4.1 Values of K in gases

Gas	K (cm ³ /gm)
CO ₂	0.229
O ₂	0.190
N ₂	0.238
He	0.196

ρ is the density and K is the Gladstone–Dale constant. This equation holds quite well for gases. The constant K is a function of the particular gas and varies slightly with wave length. Index of refraction or refractive index n is defined as $n = \frac{c_0}{c}$, where c_0 is the speed of light in vacuum and c that in the medium.

$$n = n(\rho)$$

When encountering a flow field of varying density, light passing through one part of the flow field is retarded differently from that passing through another part.

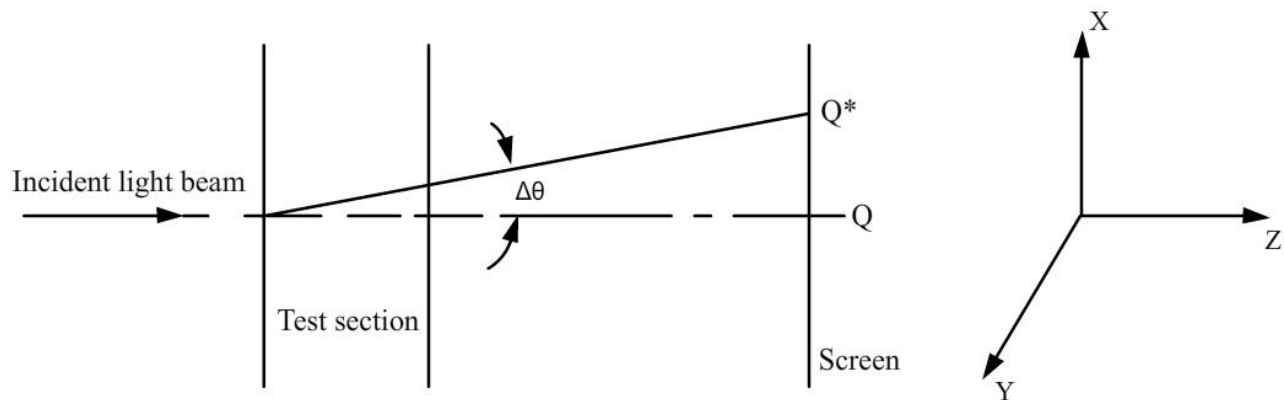


Fig.4.1 Effect of change of Refractive Index on a ray of light

As shown in Figure 4.1, light ray is deflected from original direction and reaches Q^* . Q and Q^* will coincide if at all planes normal to the incident ray n is constant. The optical path covered by the deflected ray is different from that of the undisturbed ray. It is possible to measure

- (a) displacement QQ^*
- (b) the angular deflection Δ
- (c) the path difference between the two rays

The Table 4.2 sums up the three different methods for optical flow visualisation.

Table 4.2 Comparison of the three optical methods of flow visualisation

Method	Quantity measured	Sensitive to the change of
Shadow	Displacement	$\frac{\partial^2 n}{\partial x^2}$
Schlieren	Angular deflection	$\frac{\partial n}{\partial x}$
Interferometer	Phase change	n

4.3.2 Deflection of light ray in a medium of constant density gradient

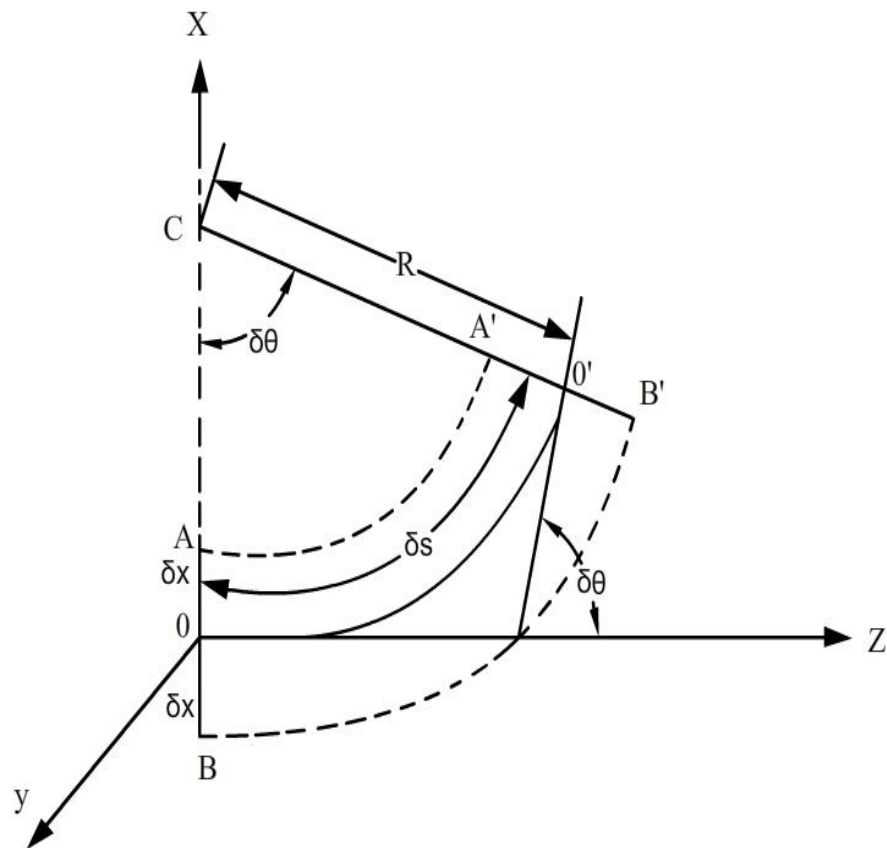


Fig.4.2: Effect of a constant gradient of refractive index on a wave front

Let OZ represent the undisturbed path of a ray of light and let A and B represent points on an element of the wave front at O. Suppose that a disturbance is introduced into the light path with a constant gradient of refractive index in the direction normal to O. If n is the refractive index at O and n_A and n_B are the refractive indices at A and B respectively then

$$n_A = n + \frac{\partial n}{\partial x} dx$$

$$n_B = n - \frac{\partial n}{\partial x} dx$$

and the corresponding optical velocities are related by the equations

$$v_A = v \frac{n}{n + \frac{\partial n}{\partial x} dx}$$

$$v_B = v \frac{n}{n - \frac{\partial n}{\partial x} dx}$$

The ray will therefore be deflected through any angle $\delta\theta$ and with a local radius of curvature R given by

$$\frac{1}{R} = \frac{1}{n} \frac{\partial n}{\partial y}$$

The total deflection θ_x in a plane normal to OY is given by

$$\theta_x = \int \frac{1}{n} \frac{\partial n}{\partial x} ds$$

and in a plane normal to OX is given by

$$\theta_y = \int \frac{1}{n} \frac{\partial n}{\partial y} ds$$

For the purpose of calculating the density it is usually assumed that the deflection from the undisturbed path is infinitesimally small so that ds may be replaced by dz in equations above.

4.3.3 The schlieren method

The set up for schlieren method which is most commonly employed is shown in Figure 3.

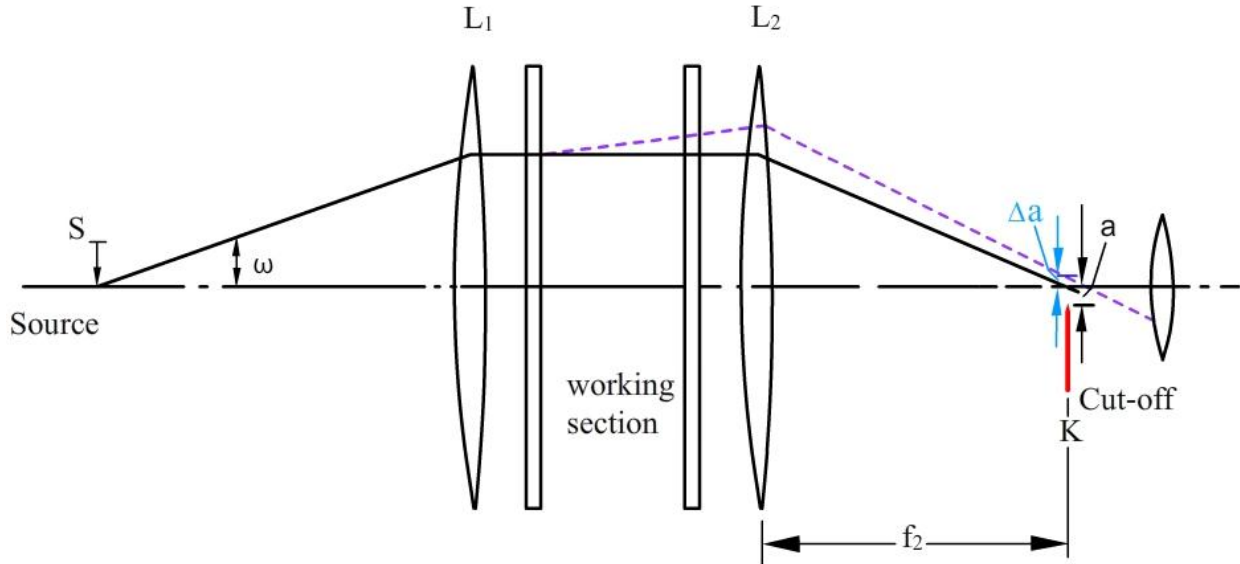
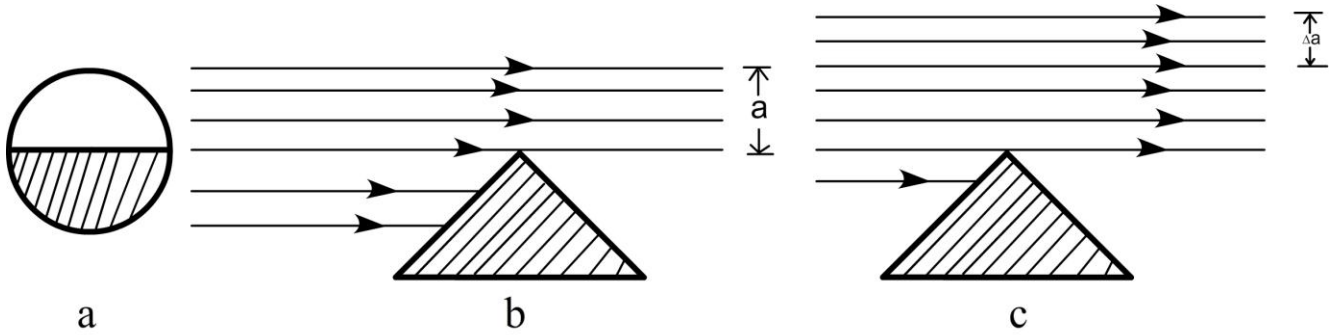


Fig.4.3 Schlieren set-up employing convex lenses

If the source is of uniform intensity and the angle ω is sufficiently small, the image obtained at the screen will be of uniform brilliance. If now an opaque cut off (knife edge) is introduced in the plane K so that a fraction of the image of the source is obscured, the illumination at the screen will remain uniform but will be reduced. In the disturbed flow part of the beam of light is deflected and the corresponding part of the image of the source moves a distance Δa relative to the cut off. This is illustrated in Figure 8.3

This movement and the change of illumination are proportional to the angular deflection θ , observations of the change of illumination will indicate the density gradient in the tunnel.



Part of the rays are cut off by the knife edge in b.
 In c, more rays reach the screen proportional to $a + \Delta a$.

Fig.4.4 Deflection of the rays of light with respect to the knife edge

Assuming θ to be small

$$\Delta a = f_2 \theta$$

The contrast is given by

$$\frac{\Delta I}{I} = \frac{\Delta a}{a}$$

where, ΔI is the change in illumination at the screen and I the original value.

Hence,

$$\frac{\Delta I}{I} = \frac{f_2 \theta}{a} = \frac{f_2}{a} \int \frac{1}{n} \frac{\partial n}{\partial x} dz$$

If high sensitivity is required the quantity 'a' will be made as small as possible.

4.3.4 Colour schlieren

It is always good to visualize flow fields of graded expansion and compressive regions using the colour schlieren arrangement. The principle of operation of colour schlieren is simple and is briefly presented in this section.

According to Gladstone Dale equation

$$n - 1 = K\rho$$

variation of K with λ is marginal

$$\frac{dn}{n} = \frac{dK}{K} + \frac{d\rho}{\rho}$$

For a compression $\frac{d\rho}{\rho}$ is + ve.

Hence, $\frac{dn}{n}$ should be + ve.

For implementing the colour schlieren, the white light is split in to its constituent colours by means of a dispersion prism. The colours in the VIBGYOR spectrum have varying values of refractive index. The value of refractive index is largest for violet and least for red.

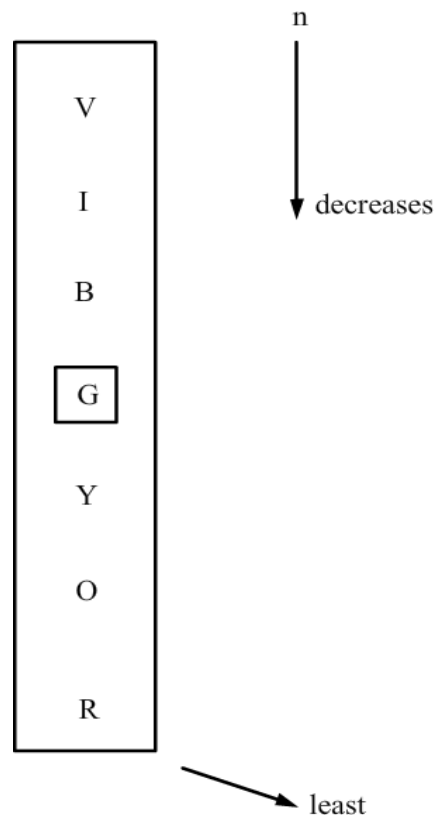


Fig.4.5 The change in refractive index with colour

Visualisation of the graded density regions can be easily obtained if the green colour is selected as the background colour.

4.3.5 Shadowgraph method

The shadowgraph method requires simpler optical apparatus than either of the other two methods. It is admirably suited to the demonstration of compressibility phenomena (particularly to the visualisation of shock waves and wakes). It is least amenable to the numerical determination of the density in the field of flow.

In its simplest form the method consists of a light source on one side of the test section and a screen on the other.

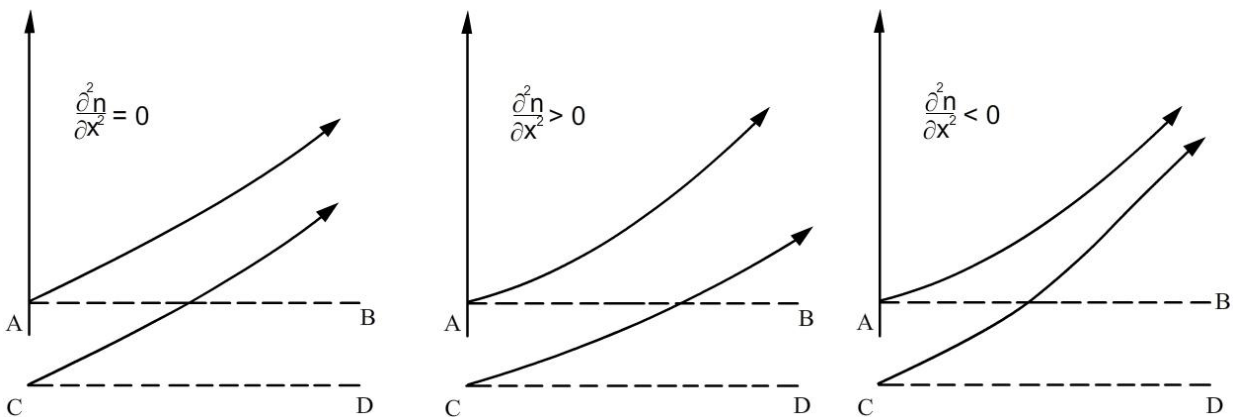


Fig.4.6 Effect of non-constant gradient of refractive index on a wave front

As shown in Fig.8.5, if the refractive index gradient $\frac{\partial n}{\partial x}$ is constant i.e. $\frac{\partial^2 n}{\partial x^2} = 0$ the deflected rays remain parallel as shown. If however $\frac{\partial^2 n}{\partial x^2}$ is positive the rays are deflected and diverge as shown. If $\frac{\partial^2 n}{\partial x^2}$ is negative deflected rays converge as shown in the Fig.4.6.

The convergence or divergence of the rays is very well understood if the bow shock in front of the blunt body in supersonic flow is observed in a shadowgraph. The shadowgraph image will have bright and dark bands as represented in Fig.8.7. In the case of the shock front, density gradients within the shock front are shown in Fig.8.8 which explains the dark and bright bands seen in the shadowgraph.

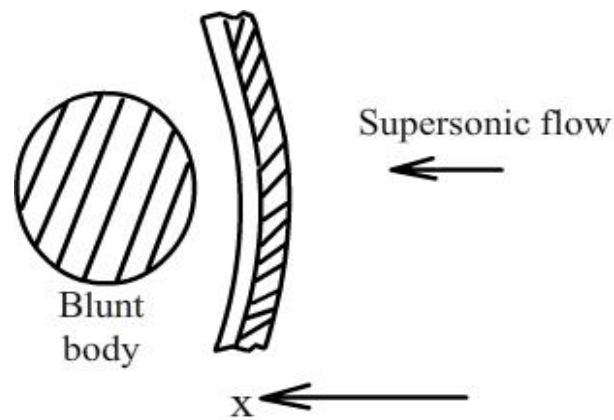


Fig.4.7 Representation of the shadowgraph ahead of a blunt body

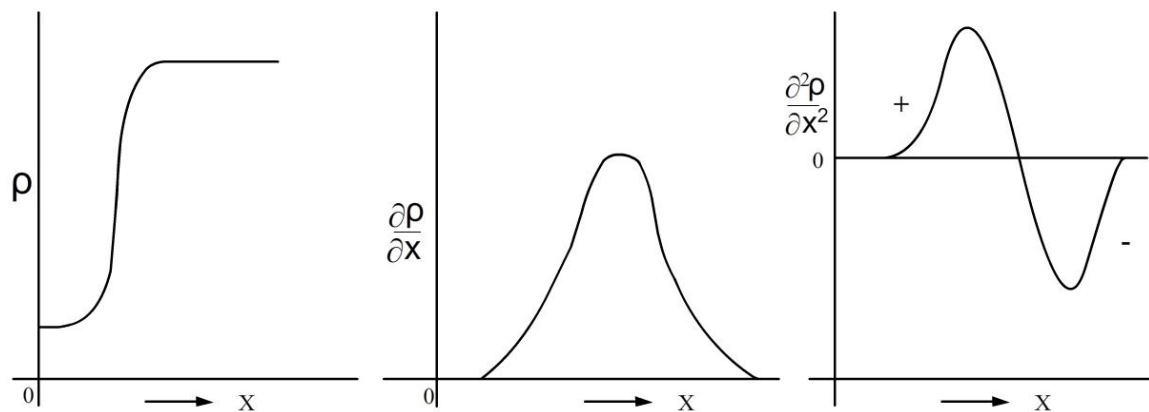


Fig.4.8 Density gradients within the bow shock

4.3.6 Interferometer method

Interference principle is illustrated in the Figure 8.9. As shown in the figure, two rays from a coherent beam reach P by two different paths. Consequently interference fringes are formed. Whether they reinforce or annul each other depends on their relative phases, which in turn depends on the lengths of their paths. If they pass through identical media the only path difference is due to the geometrical disposition.

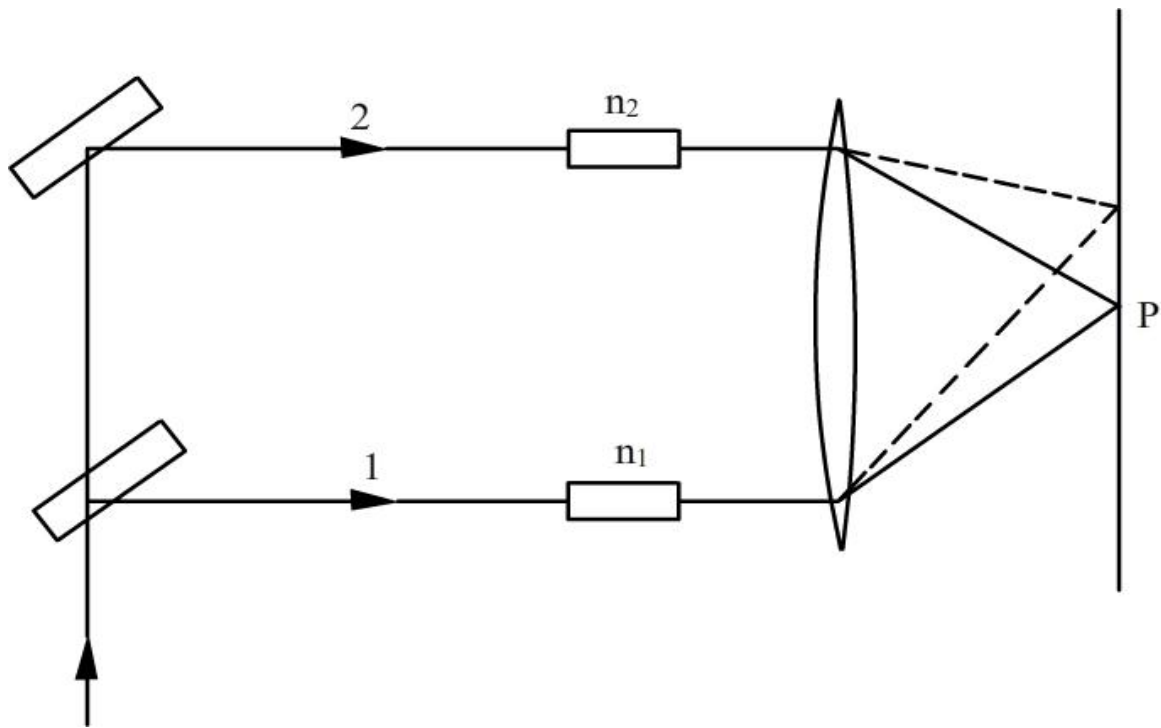


Fig.4.9 Schematic of an Interferometer

If a different medium is kept in the path of the ray (2), the effective path of that ray is changed and with it the order of interference at P. If the index of refraction in test section is increased from n_1 to n_2 the light speed is decreased from c_1 to c_2 . Additional time for traversing the test section of width L is

$$\Delta t = \frac{L}{c_2} - \frac{L}{c_1} = \frac{L}{c_0}(n_2 - n_1)$$

$L \times n$ is defined as the optical path length where L is the width of the test section. Therefore, change in optical path length

$$\Delta L = c_0 \Delta t = L(n_2 - n_1)$$

The number of interference fringes shifted

$$N = \frac{\Delta L}{\lambda} = \frac{L}{\lambda}(n_2 - n_1) = \frac{(\rho_2 - \rho_1)}{\lambda} KL$$

$$\text{Sensitivity} = \frac{N}{\Delta \rho} = \frac{KL}{\lambda} = \frac{n-1L}{\rho \lambda}$$

The sensitivity of interferometer decreases with increase in density. If a medium of different refractive index is introduced into one of the two interfering light rays, a fringe shift occurs from which the refractive index of the disturbing medium relative to the surrounding medium may be reduced. Interferometers are often used in quantitative studies. The Mach-Zender interferometer is widely employed for aerodynamic studies.

4.3.7 Glow discharge visualization for low density flows

Optical methods need a minimum level of density. In low density atmosphere, radiative characteristics of gas are employed for visualisation. The electric discharge of gas at low pressures is accompanied by the emission of light.

The method involves the acceleration of the free electrons and ions in the control volume by the electric field. Their collisions with neutral molecules produce secondary ions and electrons. These primary and secondary electrons excite gas molecules which emit radiation on spontaneous transition into the ground state. The emission intensity is a function of gas density.



SATHYABAMA

INSTITUTE OF SCIENCE AND TECHNOLOGY
(DEEMED TO BE UNIVERSITY)

Accredited "A" Grade by NAAC | 12B Status by UGC | Approved by AICTE

www.sathyabama.ac.in

School of Mechanical
Department of Aeronautical Engineering

UNIT – V - SAE1305 EXPERIMENTAL AERODYNAMICS

SAE1305 EXPERIMENTAL AERODYNAMICS

UNIT 5 MEASUREMENT TECHNIQUES

5.0 Introduction

Pressure measurement is important in many fluid mechanics related applications. From appropriate pressure measurements velocity, aerodynamic forces and moments can be determined. Pressure is measured by the force acting on unit area. Measuring devices usually indicate differential pressure i.e. in relation with atmospheric pressure. This is called gauge pressure. The measured pressure may be positive or negative with reference to the atmospheric pressure. A negative gauge pressure is referred to as vacuum.

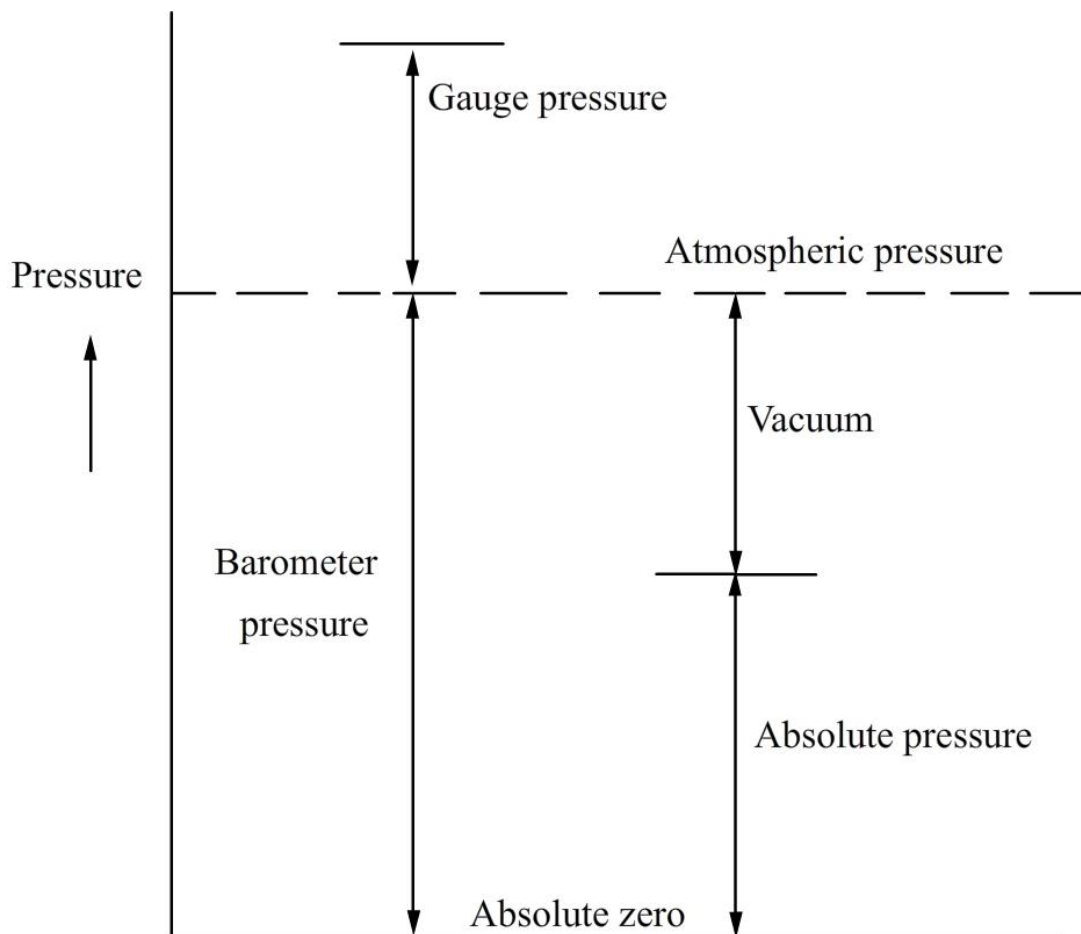


Fig.5.1 Explanation of the pressure terminology

5.1 Units of pressure

1 Pascal(1N/m ²)	= 10dyne/cm ²
1mmHg	= 133.32pascals
	= 13.595mm Water
Standard atmosphere	= 1.013 * 10 ⁵ N/m ²
1 millibar	= 1000 dyn/cm ²
1 micron	= 10 ⁻⁶ mHg
1 torr	= 1 mmHg
	= 1000micron

Absolute pressure

Absolute pressure is determined as algebraic sum of the readings of a barometer and of a manometer showing the gauge pressure. Manometers which measure absolute pressure are also available. They measure the pressure with reference to absolute zero pressure.

5.2 Pressure measuring devices

Main characteristics of manometers are pressure range, accuracy, sensitivity and speed of response. Pressure range of manometers varies from almost perfect vacuum to several hundreds of atmosphere. The conventional instruments used for pressure measurement are divided into the following groups.

- 1) Liquid column manometers
- 2) Pressure gauges with elastic sensing elements
- 3) Pressure transducers
- 4) Manometers for low absolute pressures
- 5) Manometers for very high absolute pressures

5.2.1 Liquid column manometers

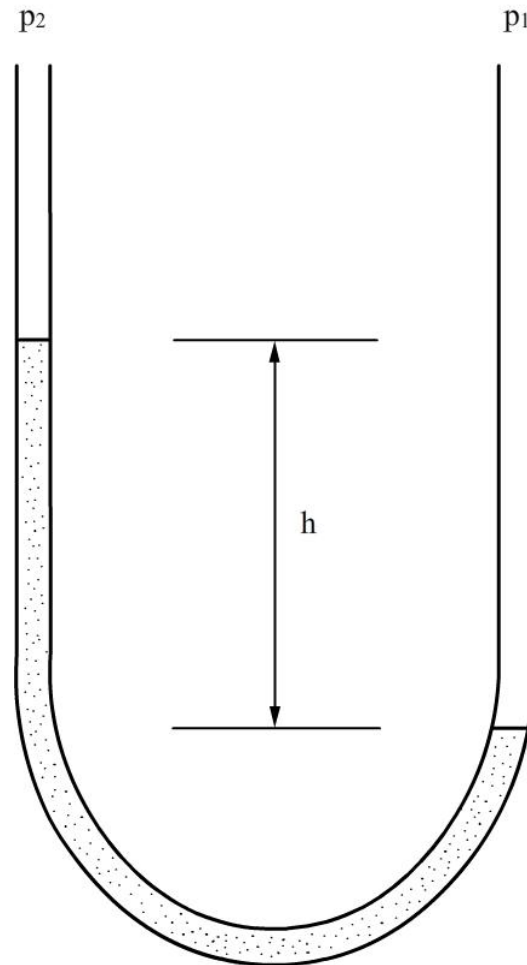


Fig. 5.2 Liquid column manometer

For amplifying the deflection in a liquid column manometer, liquids with lower density could be used or one of the limbs of the manometer may be inclined. Commonly used manometric liquids are mercury, water or alcohol. Some of the important and desirable properties of the manometric liquids are:

- High chemical stability
- Low viscosity
- Low capillary constant
- Low coefficient of thermal expansion
- Low volatility
- Low vapour pressure

High thermal stability and low volatility are important for maintaining a constant. Specific gravity. High viscosity causes transmission lags .Thermal expansion causes changes in zero reading. While measuring low pressures, vapour pressure of the manometric fluid is an important consideration. Properties of some of the commonly used fluids are given in the Table 5.1.

Table 5.1 Typical properties of manometric fluids

Fluid	Specific gravity	B.P.(°C) at 760mm Hg	Surface Tension dyn/cm	Viscosity C_P	Coeft.of Volumetric Expansion *10⁵
Methyl Alcohol	0.792	64.7	22.6	0.59	
Ethyl Alcohol	0.789	78.4	22.0	1.9	110
Mercury	13.55	356.59	465	1.55	18
Toluene	0.866	110.8	28.4		
CCl₄	1.594	76.8	26.8	0.97	

5.2.2 Inclined manometer

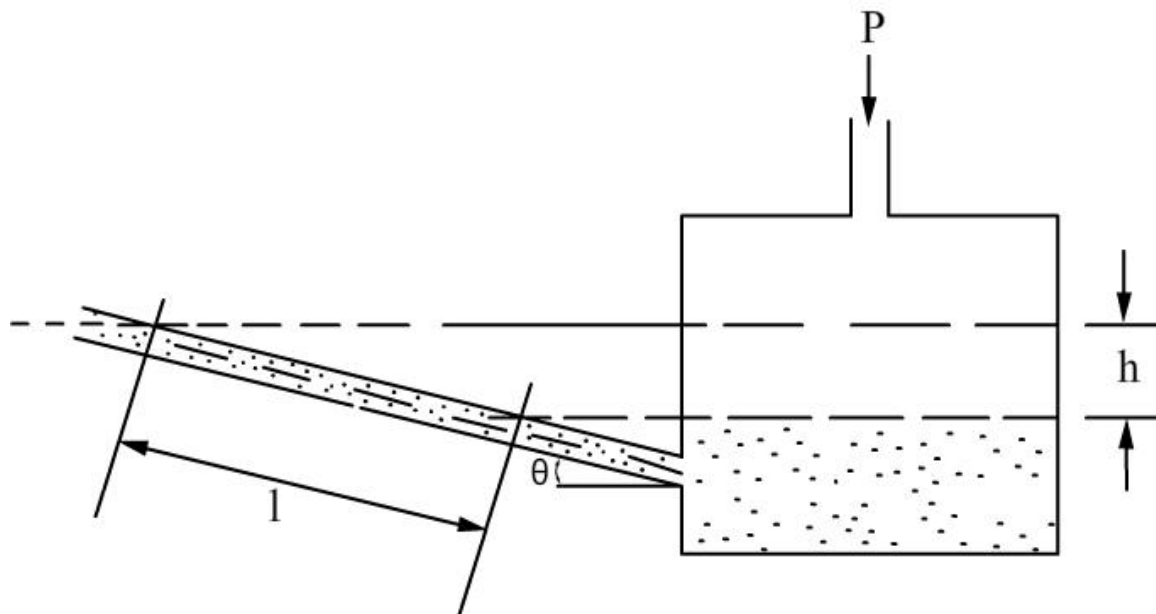


Fig. 5.3 Inclined manometer

The Figure 5.3 shows the amplification of the reading of applied pressure ‘h’ as

$$\frac{h}{l} = \sin \theta$$

5.2.3 Mercury barometer

Barometer is the device used to measure the atmospheric pressure. Mercury barometer consists essentially of a glass tube sealed at one end and mounted vertically in a bowl or cistern of mercury so that the open end of the tube is submerged below the surface of mercury in the cistern. In the Fig.5.4 (i) the zero level of mercury in the cistern is shown under the influence of atmospheric pressure p_1 . When $p_2=p_1$ = atmospheric pressure, the zero level in the cistern can be marked. If the tube is open and if different pressures act in the cistern and in the tube, then there will be difference in the levels of mercury. If p_1 is greater than p_2 as shown in Fig.5.4 (ii), then mercury will be forced down in the cistern and corresponding rise will be there in the tube.

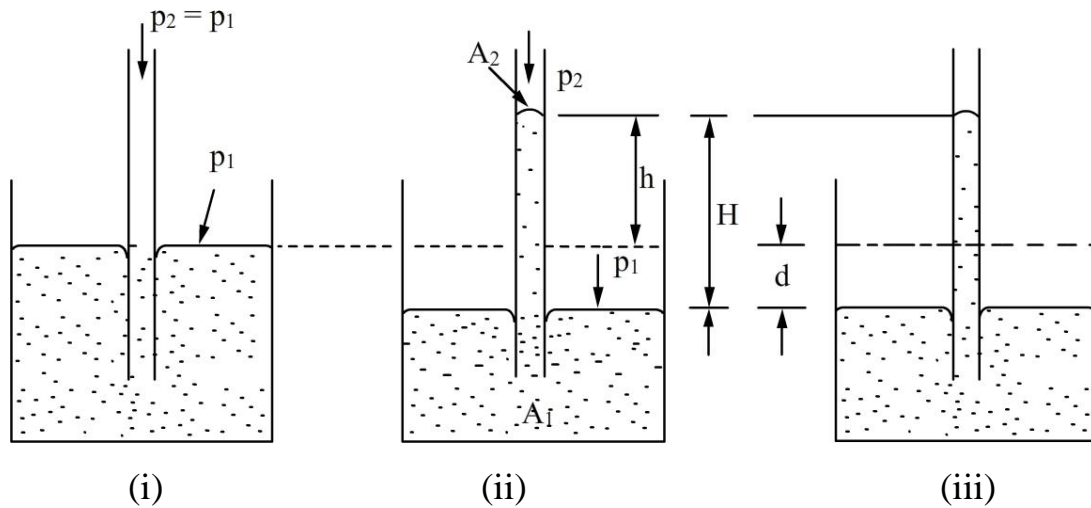


Fig. 5.4 Principle of mercury barometer

The balance of pressures will be given by $p_1 = p_2 + H\rho$ 5.1

(where H is the difference between levels of mercury in the cistern and in the tube and ρ the density of mercury). From the Figure 5.4 (ii), $H=h+d$

The quantity of mercury that has left the cistern is same as that has risen in the tube.

$A_1 d = A_2 h$ where A_1 and A_2 are areas of the cistern and the tube respectively.

$$d = \frac{A_2}{A_1} h$$

$$\begin{aligned} \therefore H &= h + h \left(\frac{A_2}{A_1} \right) \\ &= h \left(1 + \frac{A_2}{A_1} \right) \dots\dots\dots 5.2 \end{aligned}$$

Replacing H in equation 5.1

$$p_1 = p_2 + h \left(1 + \frac{A_2}{A_1} \right) \rho \dots\dots\dots 5.3$$

$p_2 \rightarrow 0$ in practical cases as the tube will be evacuated and sealed.

$$p_1 = h \left(1 + \frac{A_2}{A_1} \right) \rho \dots\dots\dots 5.4$$

5.2.4 Micromanometer

For accurate measurement of extremely small pressure differences micromanometers are used. In the Figure 5.5 the instrument is initially adjusted such that $p_1 = p_2$.

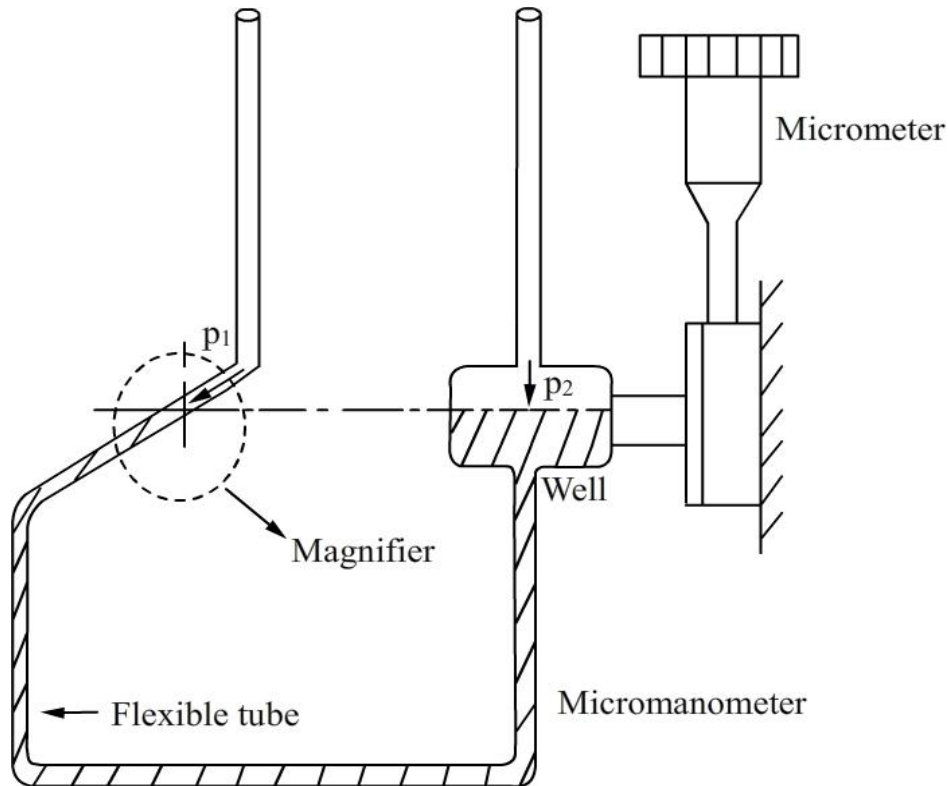


Fig. 5.5 Typical Micromanometer

The meniscus in the inclined tube is located at a reference level fixed by the hairline viewed through the magnifier. The reading of the micrometer is noted. Application of the unknown pressure difference causes the meniscus to move off the hairline but it can be restored to the initial position by raising or lowering the well (mercury sump). The difference in the initial and final micrometer readings gives the height of the mercury column and hence the pressure. Pressures as low as 0.025mm water column can be measured.

5.3 Mechanical manometers

Mechanical manometers provide faster response than liquid column manometers. In liquid column measurements, lag is due to the displacements of the liquid. In elastic sensing element type of manometers the time lag is due to the time required for equalisation of pressure to be measured with that in the sensing chamber. The deformation of elastic sensing elements is measured with the aid of kinematic, optical or electrical systems. There are three types of elastic sensing elements which are (i) Bourdon Tubes (ii) Diaphragms (flat or corrugated) (iii) Bellows

5.3.1 Bourdon tube

Bourdon tube is the oldest pressure sensing element .It is a length of metal tube of elliptical cross section and shaped into letter 'C'.

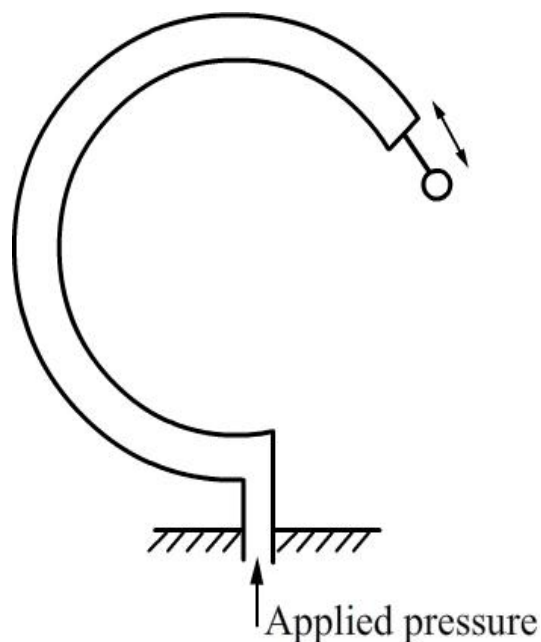


Fig.5.6 Bourdon tube pressure gauge

One end is left free and the other end is fixed and is open for the pressure source to be applied. A tube of elliptical cross section has a smaller volume than a circular one of the same length and perimeter. When connected to the pressure source it is made to accommodate more of the fluid. Resultant of all reactions will produce maximum displacement at the free end. Within close limits, the change in angle subtended at the centre by a tube is proportional to the change of internal pressure and within the limits of proportionality of the material; the displacement of the free end is proportional to the applied pressure.

The ratio between major and minor axes decides the sensitivity of the Bourdon tube. The larger is the higher is the sensitivity. Materials of the Bourdon tube is Phosphor bronze, Beryllium bronze or Beryllium Copper.

5.3.2 Elastic diaphragms

The pressure sensors making use of elastic diaphragms consist of a diaphragm fixed in a tubular member. The pressure to be measured is applied on one side. The mathematical relation between pressure and central deflection for a flat circular diaphragm is given by

$$p = \frac{16Et^4}{3a^4(1-\mu^2)} \left[\frac{y_c}{t} + 0.488 \left(\frac{y_c}{t} \right)^3 + \dots \right] \dots\dots\dots 5.5$$

To have a linear pressure deflection relation, the second and later terms should be small.

p = applied pressure

t = thickness

a = radius

y_c = central deflection

E = Youngs modulus

μ = Poisson's ratio → $\frac{\text{lateral strain}}{\text{Axial strain}}$

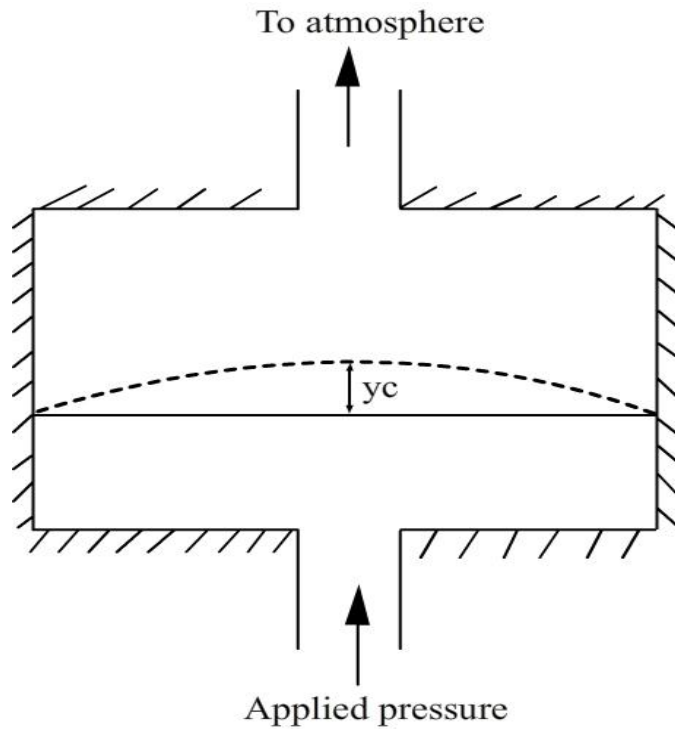


Fig.5.7 Diaphragm pressure gauge

As seen from the equation the pressure deflection relation is not linear. If a non-linearity of 5% is acceptable the deflection must be less than 1/3 of thickness. Neglecting the higher order terms within brackets,

$$p = \frac{16Et^4}{3a^4 \pi(1-\mu^2)} \times \frac{y_c}{t}$$

$$p = \frac{16Et^3 y_c}{3a^4(1-\mu^2)}$$

$$\frac{y_c}{p} = \frac{\cancel{y_c} 3a^4(1-\mu^2)}{16Et^3 \cancel{y_c}} \dots\dots\dots 5.6$$

$$\frac{y_c}{p} = K = \frac{3(1-\mu^2)a^4}{16E t^3} \dots\dots\dots 5.7$$

where 'K' is the sensitivity of the device.

The natural frequency of the diaphragm may be written as follows:

$$\omega = 10.2 \left[\frac{E}{12\rho_d(1-\mu^2)} \right]^{1/2} \frac{t}{a^2} \text{ rad/s} \dots\dots\dots 5.8$$

Diaphragm has infinite number of natural frequencies and the lowest of them is considered here. From the two equations for sensitivity ‘K’ and the natural frequency ω .

Sensitivity (K) and natural frequency (ω) are related by

$$\frac{y_c}{p} = K = \frac{1.63}{\omega^2 t \rho_d} \dots\dots\dots (5.9)$$

(ρ_d is density of diaphragm material)

Sensitivity is inversely proportional to square of natural frequency. Sensitivity can be improved by lowering the natural frequency. The natural frequency should be 3 to 4 times the frequency of pressure pulsations. Compared to bourdon tubes diaphragms have higher natural frequencies. Hence, they can be used for the measurement of dynamic pressures of higher frequency fluctuations. They can be installed flush with the surface of the body and hence there is only much less transmission lag.

5.3.3 a) Corrugated diaphragms

Corrugated diaphragms permit considerably larger deflections than flat diaphragms. Their number and depth control the response and sensitivity. The greater the number and depth, the more linear is its deflection and greater is the sensitivity.

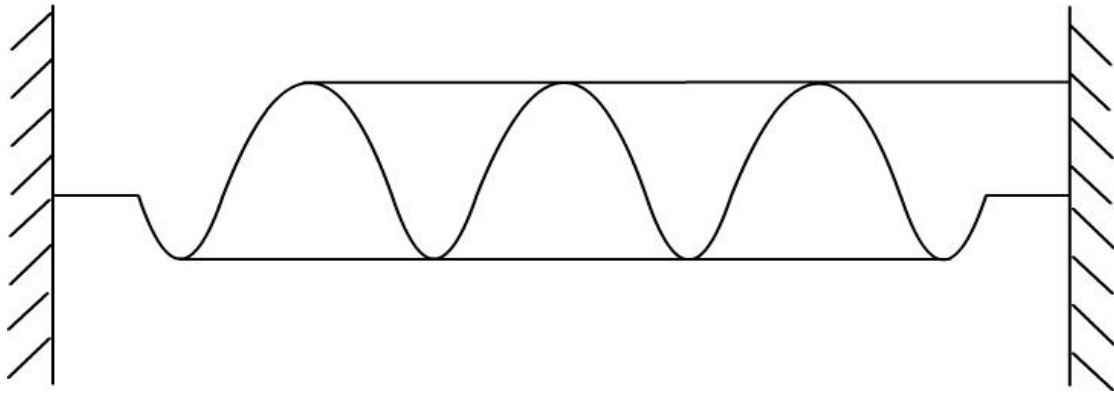


Fig. 5.8 Corrugated diaphragm

5.3.3 (b) Capsules, Bellows

For even larger deflections than the diaphragms corrugated diaphragms are made in to boxes or bellows. Bellows are most commonly used to measure small steady pressures.

5.4 Pressure Transducers

5.4.1 Diaphragm type pressure transducers

They convert the pressure to be measured into electrical signals. For example, pressure transducers whose operating principle is based on measuring changes in inductive, capacitive or ohmic resistances caused by the deformation of an elastic element.

$$\text{Capacitance } C = \epsilon_a a / d \dots\dots\dots 5.10$$

where $\epsilon_a \rightarrow$ absolute permittivity

$$\frac{\epsilon_a}{\epsilon_0} = K \frac{1}{4\pi \times 9 \times 10^9 \text{ E/m}}$$

a = area of plates

d = distance between the plates

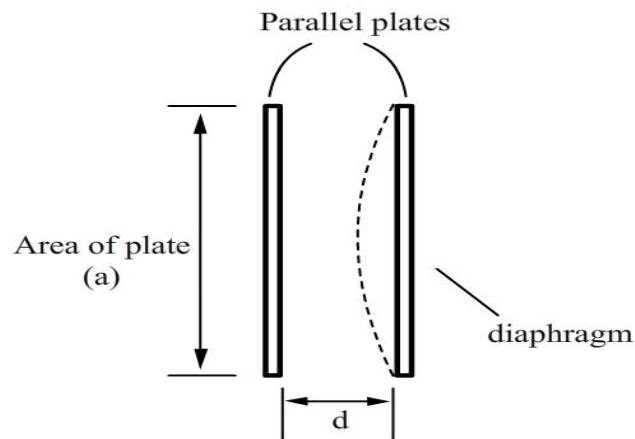


Fig.5.9 Elastic diaphragm used in a parallel plate capacitor

With the application of pressure, the diaphragm deforms with the central deflection as shown. This changes the capacitance in an electrical circuit which can be calibrated against pressure to be measured.

5.4.2 Piezo-Electric pressure transducers

The word piezo-electric is derived from the Greek word “piezein” meaning squeeze or press. Certain materials possess the ability to generate electrical potential when subjected to mechanical strain. Conversely, they change dimensions when supplied with voltage. The potential developed by application of stress is not held under static conditions. Dynamic pressures in the range of frequencies from kHz to 100MHz can be measured using piezo-electric transducers. The use of piezo-electric effect is limited to dynamic measurements. Some materials exhibiting piezo electric properties are quartz, tourmaline, barium titanate, and Lead zirconate. Quartz is the preferred material, as it possesses good mechanical properties. Also, it is a good insulator least influenced by moisture.

5.4.3 Pressure Sensitive Paints (PSP)

They are composed of luminescent molecules dispersed in Oxygen permeable polymer binder. When PSP is exposed to blue or an ultraviolet light the luminescent molecules are excited to a higher energy level.

From this excited state they can discharge in three ways:

- (i) by discharging light
- (ii) by transferring energy to the polymer binder(heating)
- (iii) colliding with Oxygen molecules.

Since the luminescent molecules react with Oxygen they collide and release light at the same time. The amount of light emitted is inversely proportional to the amount of Oxygen molecules on the surface.

5.5 Measurement of high pressures

5.5.1 Electrical resistance gauges – principle of operation

Bourdon Tube or strain gauge can be used for high pressures. Very high pressures (say above 1000bars) may be measured by means of electrical resistance gauges which are known as **Bridgeman gauge**. By way of principle of operation, they make use of resistance change brought about by direct application of pressure to the conductor itself. Referring to the Figure, the sensing element is the thin wire of Magnanin (84 Cu + 12 Mn + 4 Ni) or an alloy of Gold and Chromium (2.1%) which is loosely wound. When pressure is applied, bulk compression effects produce a change in resistance which may be calibrated against pressure. The general relation between electrical and mechanical may be derived as follows:

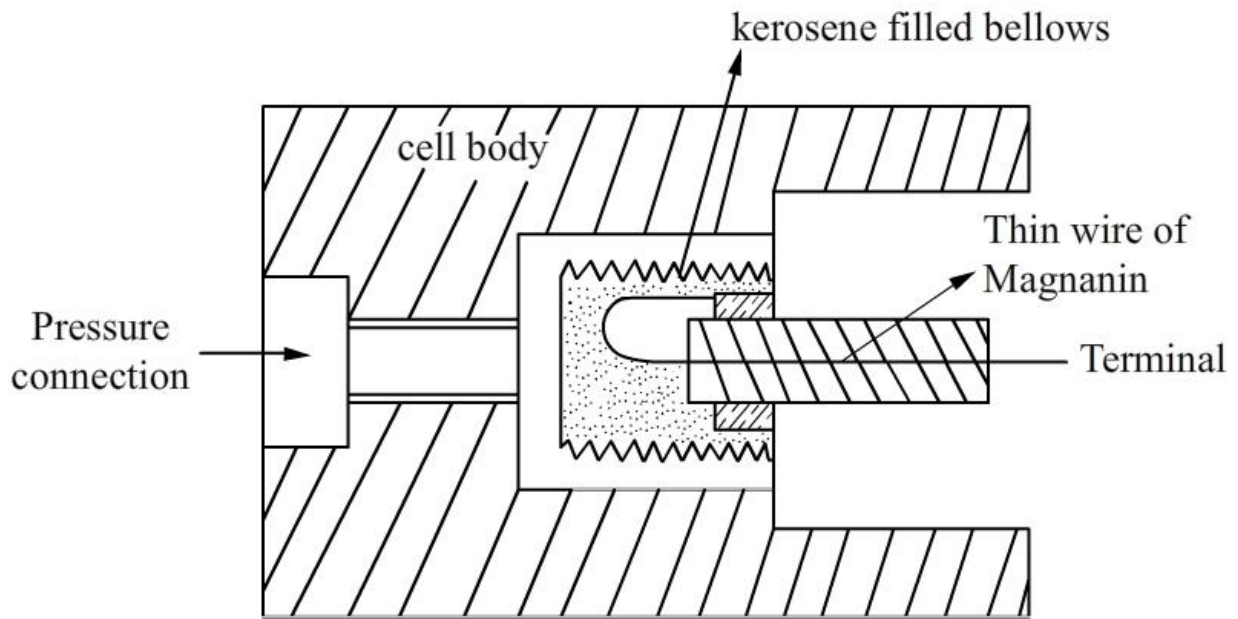


Fig.5.10 Sensor of a Bridgemans Gauge

$$R = \frac{\rho L}{A} = \frac{\rho L}{CD^2} \dots\dots\dots(5.11)$$

R = Resistance, ohms

L = Length of conductors

A = Area = CD^2

where D is the diameter of the circular conductor and C a constant

ρ = Resistivity ohm cm

If the conductor is strained each of the quantities in the equation will change.

Differentiating

$$dR = \frac{CD^2(Ldp + \rho dL) - 2C\rho DLdD}{(CD^2)^2}$$

$$= \frac{1}{CD^2} \left[(Ldp + \rho dL) - 2\rho L \frac{dD}{D} \right] \dots\dots\dots 5.12$$

Dividing (5.12) by (5.11) gives

$$\frac{dR}{R} = \frac{dL}{L} - \frac{2dD}{D} + \frac{dp}{\rho}$$

The wire will be subjected to biaxial stresses because the ends in providing electrical continuity will not be subjected to pressure.

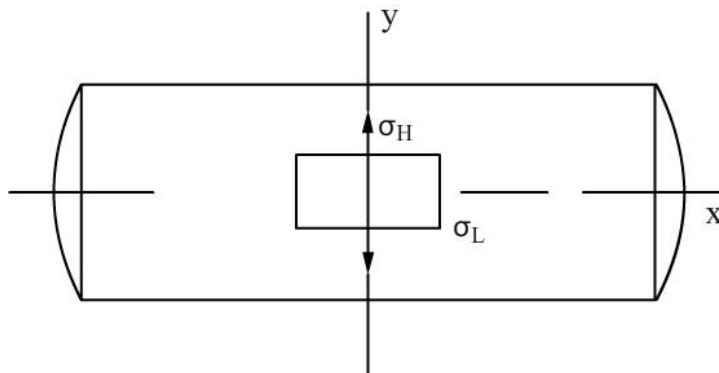


Fig.5.11 Bi-axial stresses on a small element

Let us consider a general element subjected to stresses which may be denoted as σ_x and σ_y . Suppose σ_x and σ_y are applied one at a time. If σ_x is applied first, there will be strain in the

$$x - \text{direction} = \frac{\sigma_x}{E}$$

Because of Poisson's effect, the strain in y direction = $-\mu \frac{\sigma_x}{E}$

If σ_y is applied first

$$\text{Strain in y direction} = \frac{\sigma_y}{E}$$

$$\text{Strain in x direction} = -\mu \frac{\sigma_y}{E}$$

There will be a net strain of

$$\epsilon_x = \frac{1}{E}(\sigma_x - \mu\sigma_y)$$

$$\epsilon_y = -\frac{1}{E}(\sigma_y - \mu\sigma_x)$$

Stresses are nothing but applied pressure

$$\sigma_x = \sigma_y = -p \quad \text{assuming } \sigma_z = 0$$

Lateral Strain

$$\epsilon_x = \epsilon_y = \frac{dD}{D} = -\frac{p}{E}(1-\mu)$$

$$\epsilon_z = \frac{dL}{L} = 2\mu \frac{p}{E}$$

Biaxial stress situation is assumed.

Longitudinal Strain

$$\begin{aligned} \therefore \frac{dR}{R} &= \frac{dL}{L} - \frac{2dD}{D} + \frac{dp}{\rho} \quad (\text{Substitute from above}) \\ &= 2\mu \frac{p}{E} + 2\frac{p}{E}(1-\mu) + \frac{dp}{\rho} \\ &= \frac{2p}{E} + \frac{dp}{\rho} \end{aligned}$$

If specific resistance ρ does not depend on pressure $\frac{dp}{\rho}$ can be neglected.

$$\frac{dR}{R} = 2\frac{p}{E}$$

$R = R_0(1 + bp)$ where, $b = 2 / E$.

$$\frac{dR/R}{p} = \frac{2}{E} + \frac{dp/p}{\rho} \dots\dots\dots 5.13$$

where b is called pressure coefficient of resistance. Resistance varies linearly with pressure.

5.6 Ranges of different manometers

Liquid column manometers	10 – 0.5 x 10 ⁶ pascals
Bourdon tubes	Vacuum to a few thousand bars
Diaphragms	Vacuum to a few hundred bars
Bellows	Vacuum to a hundred bar

5.7 Measurement of vacuum

Pressures below atmosphere is vacuum. Very low pressures may be defined as below 1mmHg.

Ultra low pressures is less than a milli micron (<10⁻³micron)

Measurement of vacuum may be by two methods

Direct measurement

Resulting in a displacement caused by the action of force [Spiral Bourdon tubes, flat or corrugated diaphragm, capsules and various other manometers]

Indirect measurement or inferential methods

Pressure is determined through the measurement of certain pressure controlled properties such as volume, thermal conductivity etc.

5.7.1 Inferential methods

a) McLeod gauge

The working of McLeod Gauge is based on Boyles' fundamental equation.

$$p_1 = \frac{p_2 V_2}{V_1}$$

where p and V refer to pressure and volume respectively and subscripts 1 and 2 refer to initial and final conditions. Conventional McLeod gauge is made of glass. Refer to Fig. 5.12. It consists of the capillary 'C', bulb 'B' and the mercury sump which is connected to the lower end of the glass tube such that it can be moved up and down.

The pressure to be measured (the unknown pressure) is connected to the upper end of the glass part. When the mercury level in the gauge is below the cut off 'F', the unknown pressure fills the gauge including the bulb B and capillary C. When the mercury sump is moved up, the level in the gauge rises and when it reaches the cut off 'F' a known volume of gas at pressure to be measured is trapped in bulb B and capillary C.

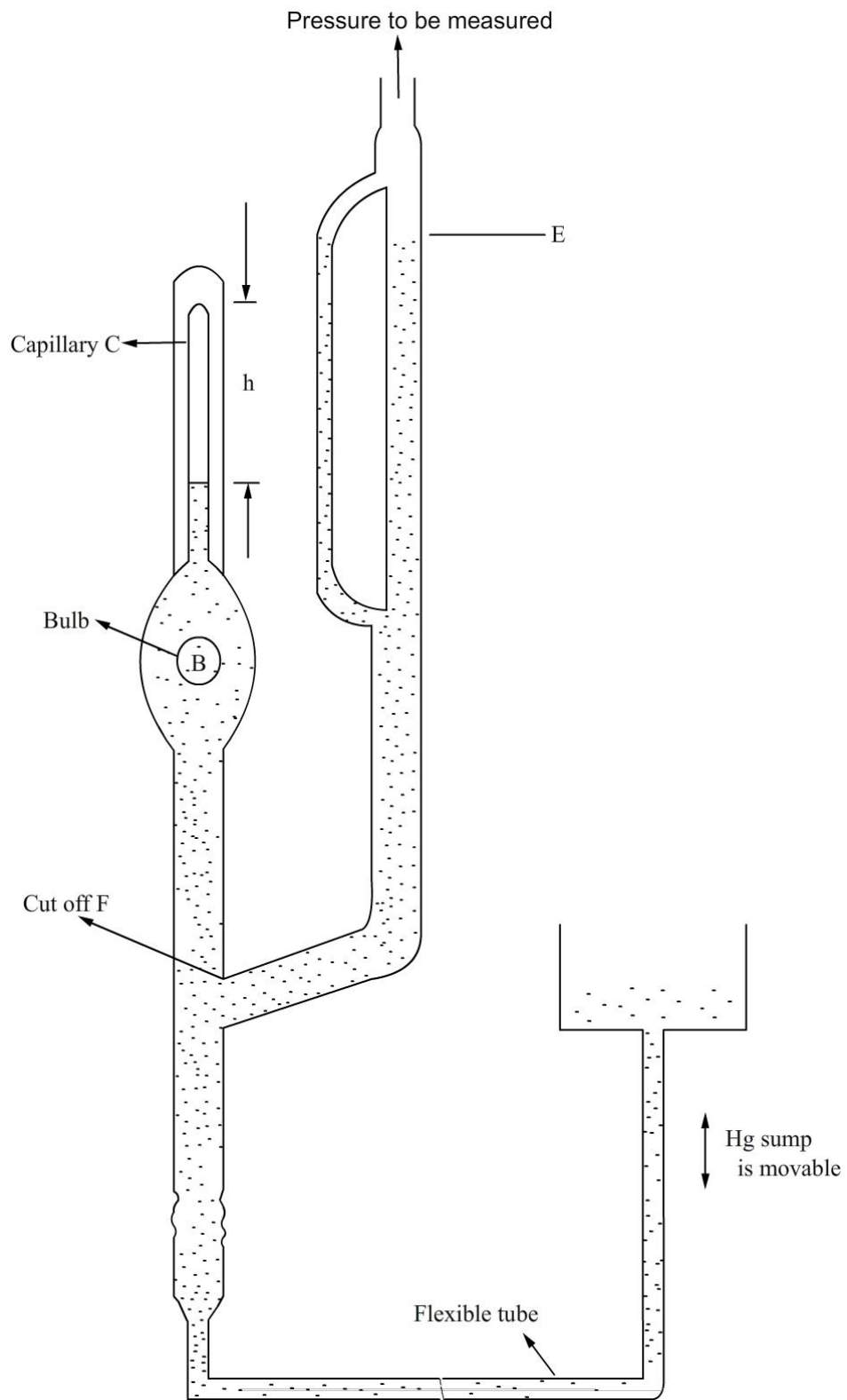


Fig.5.12 McLeod gauge

Mercury is then forced up into the bulb and capillary. Assume the sump is raised to such a level that the gas at the pressure to be measured which filled the volume above the cut off is now compressed to the volume represented by the column h.

Suppose the original volume after then mercury reaches F is V_0 . This is at a pressure being measured p_1

$$\begin{aligned}V_0 \times p_1 &= ah \times (p_1 + h) \\ &= p_1 ah + ah^2\end{aligned}$$

$$V_0 p_1 - p_1 ah = ah^2$$

$$p_1 (V_0 - ah) = ah^2$$

As 'ah' is $\lll V_0$ it is neglected.

$$p_1 = \frac{ah^2}{V_0}$$

Applications of McLeod gauge

McLeod gauge is used mainly for calibrating other inferential type of gauges. The shortcomings of the McLeod gauge are its fragility and the inability to measure continuously. The vapor pressure of Mercury sets the lower limit of measurement range of the gauge.

b) Thermal conductivity gauges

The working principle of thermal conductivity gauges is that at low pressures heat lost by a heated object by conduction through molecules will depend on pressure. This is valid only for certain pressure range.

When the mean free path is comparable with the dimensions of the gauge head the heat loss from a heated wire in the gauge head will be by (i) conduction through leads (ii) radiation to surroundings (iii) conduction through molecules.

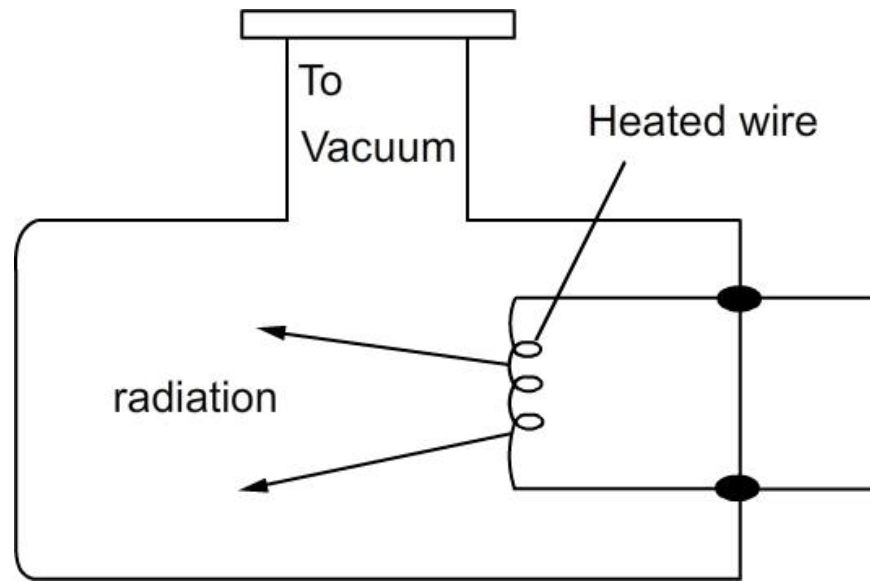


Fig.5.13 Gauge head of the thermal conductivity gauge

The range of thermal conductivity gauges is from mm of Hg to 10^{-3} mmHg. At higher pressures, heat loss from the heated wire is insensitive to the pressure change. At lower pressure heat loss by (i) and (ii) become more significant. There are two kinds of the thermocouple gauges.

c) Pirani gauge

Measures change in resistance of the heated wire when it loses heat to the gas molecules in the gauge head. In this case the gauge is called pirani gauge.

d) Thermocouple gauge

Instead of measuring electrical resistance, a thermocouple is kept in contact with the heated wire and the temperature of the wire is directly measured as a measure of pressure.

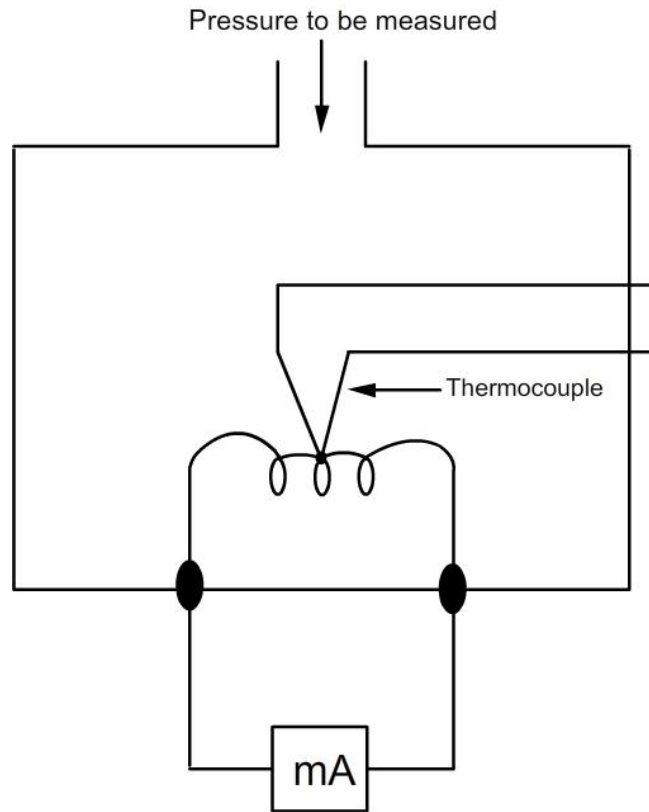


Fig.5.14 Thermocouple gauge head

e) Hot cathode ionisation gauges

At higher levels of vacuum, the measurement of pressure is by using Ionisation gauges. They operate on the principle of ionising the gas by means of electrons emitted by a heated filament. The kinetic energy acquired by an electron in passing through a potential difference of V volts corresponds to a value equal to $V \cdot e$ where e is the charge of the electron. When this energy exceeds a certain critical value corresponding to the ionization potential V_i , there is a possibility that collisions between molecules and electrons will result in the formation of +ve ions. The relatively high velocity electrons on hitting a gas molecule drives an electron out of it leaving it positively charged. For gases such as N_2 , O_2 etc, V_i is ~ 15 volts. The measurement of the ions produced is a measure of the pressure. The electrons are speeded up by an electric field and +ve ions produced are collected. The number of +ve ions formed will depend on the number of molecules and therefore on the pressure.

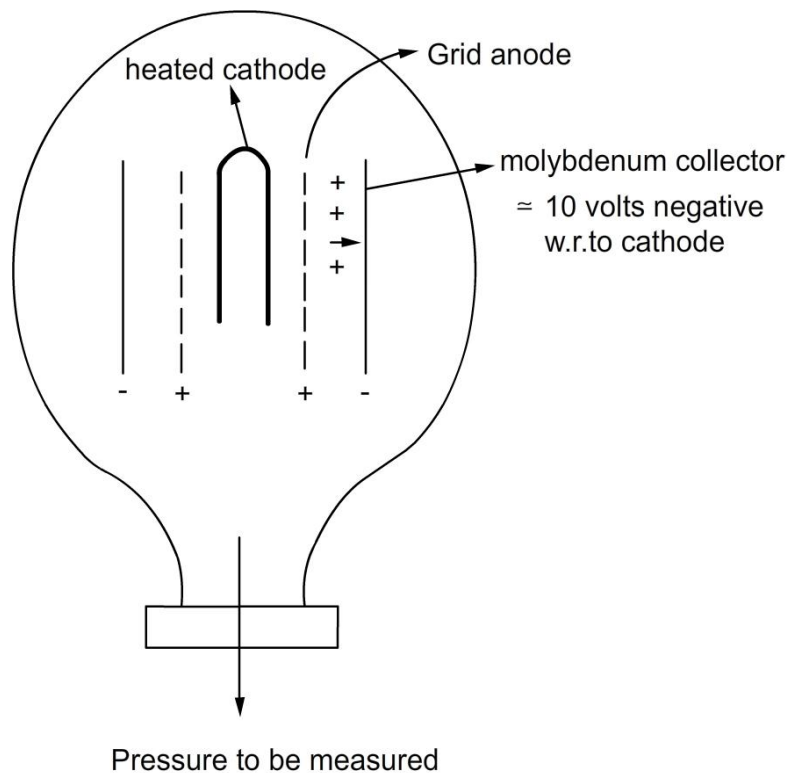


Fig.5.15 Ionisation gauge

The gauge consists of a cathode, grid anode and a negative plate. The negative plate is at $\sim 10\text{V}$ negative with respect to the cathode. The electrons emitted by the hot cathode (filament) are speeded up by the electric field and the positive ions produced are collected by the negative plate.

g) Cold cathode ionisation gauge (Penning gauge)

This gauge also works on the ionization principle. Positive ions are produced by the electrons and current due to these ions gives a measure of the pressure. Electrons are ejected from a cold cathode of Zirconium, Thorium by electric discharge. The gauge consists of two plate cathodes and a ring anode . A potential difference of $\sim 2\text{KV}$ is applied across the electrodes.

The travel of electrons is made over a much longer distance. The secondary electrons are made to travel in helical paths before reaching the anode. This is accomplished by a magnetic field.

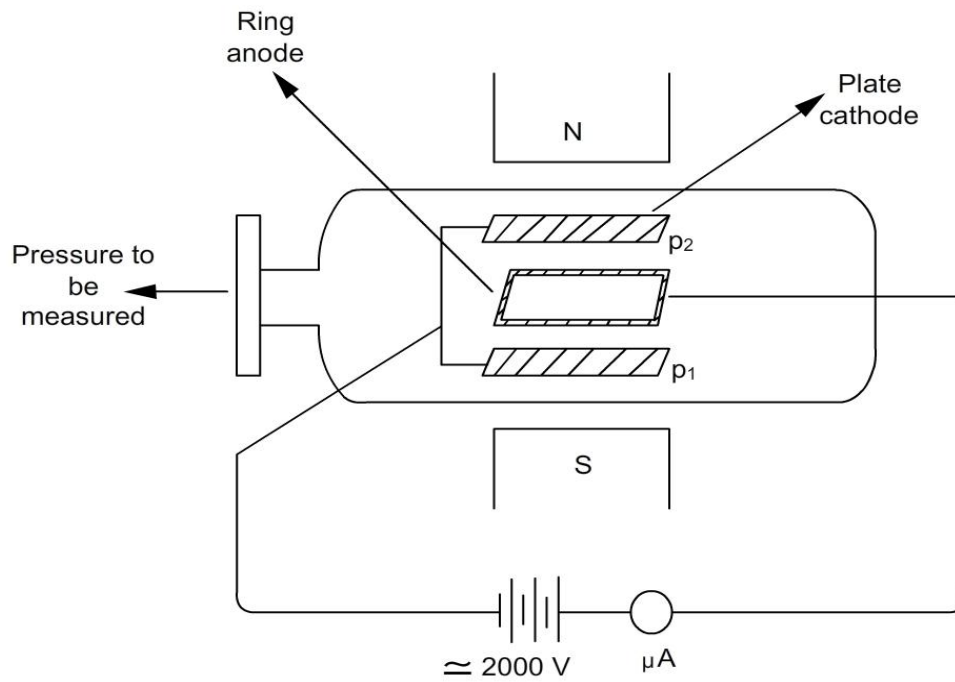


Fig.5.16 Cold cathode ionization gauge

Magnetic poles are kept such that the flux with lines of force is applied perpendicular to the two cathodes.

5.8 Measurement of pressure in flows

In flows, distinction has to be made between static and stagnation pressures.

Static pressure

Pressure acting on the surface of a body imagined to be moving with the fluid with the same velocity as the medium is the static pressure.

Stagnation pressure

It is the pressure of a fluid imagined to be brought to rest isentropically.

5.8.1 Measurement of static pressure

Common technique is to connect a probe to an orifice drilled perpendicular to the wall of the model where the streamlines are undistorted and parallel.

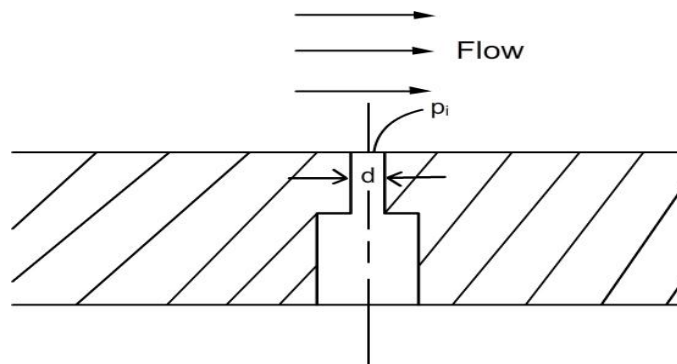


Fig.5.17 Static pressure orifice (tap) on a flat wall

Static hole diameter is about 1/5 of the boundary layer thickness. Practically the diameter is about 0.25mm on small models and 2.5mm on larger installations. The correctness of the static pressure measured is dependent on 'd' the orifice diameter [Fig.5.17]. The influence of the orifice diameter on the error in static pressure measurements is given graphically in Fig.5.18.

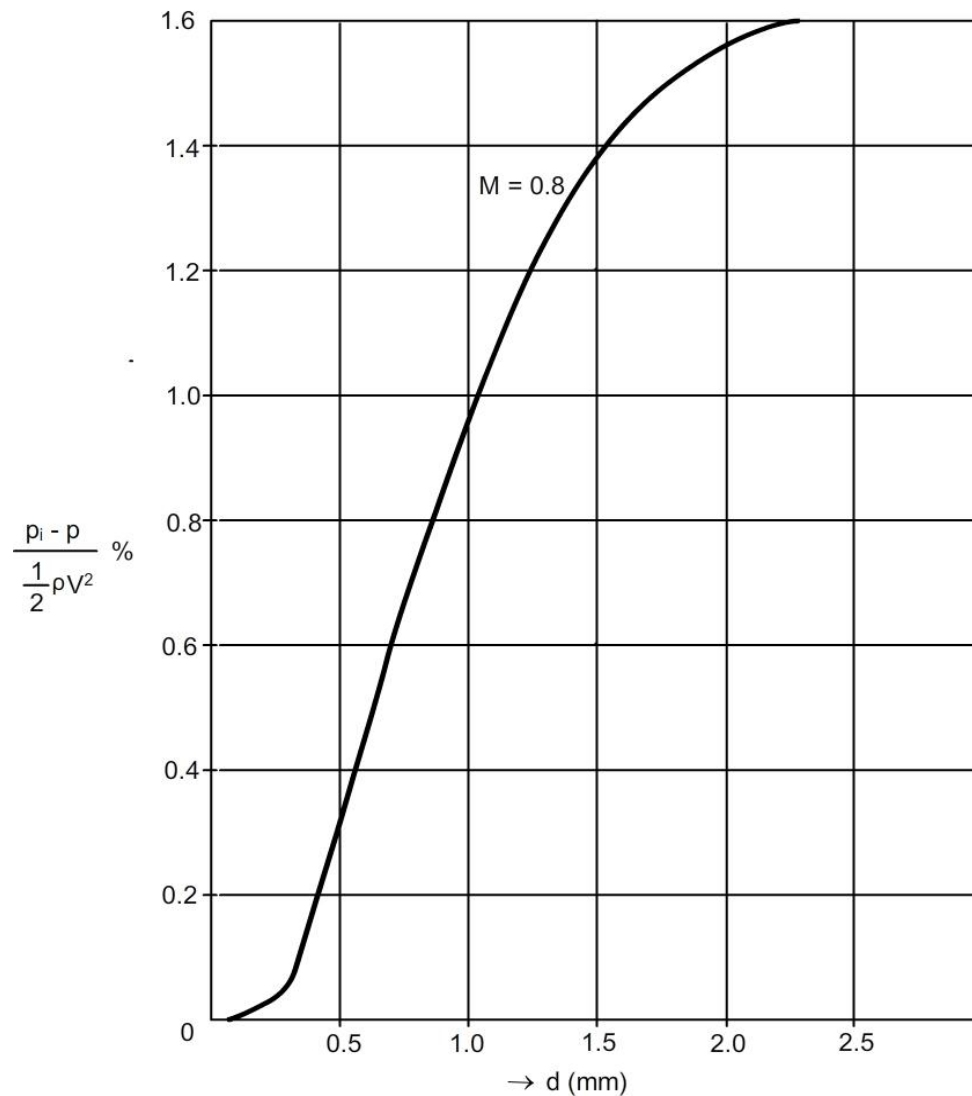


Fig.5.18 Influence of error on orifice diameter

The static pressure orifices (taps) on the walls of the flow channel provide the wall static pressure. The wall static pressure can not be assumed to prevail inside the flow. In order to get the pressure inside the flow, probes of suitable design have to be made use of.

5.8.2 Static pressure probes for subsonic flow

The commonly used static pressure probe in subsonic flows is the Prandtl probe. The Prandtl probe is an intrusive device. The pressure sensing orifices on the periphery of the probe are carefully located such that the influence of the nose and stem of the probe nullify each other.

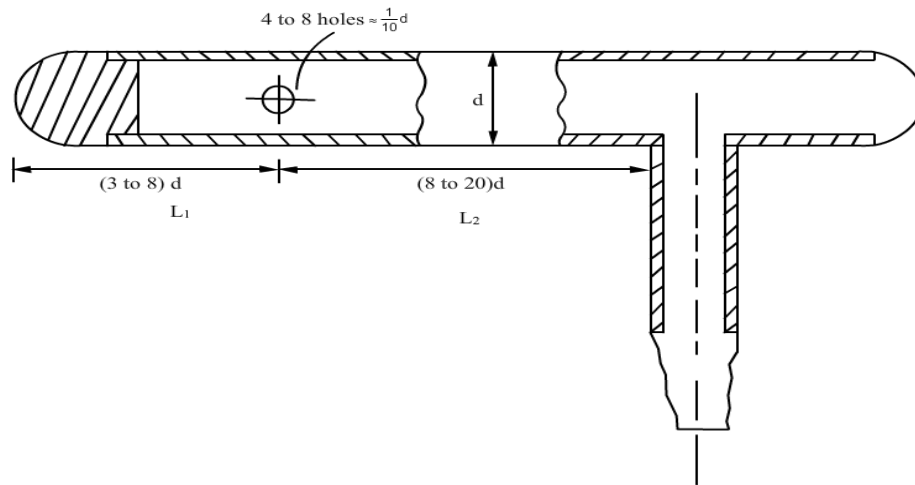


Fig.5.19 The Prandtl probe

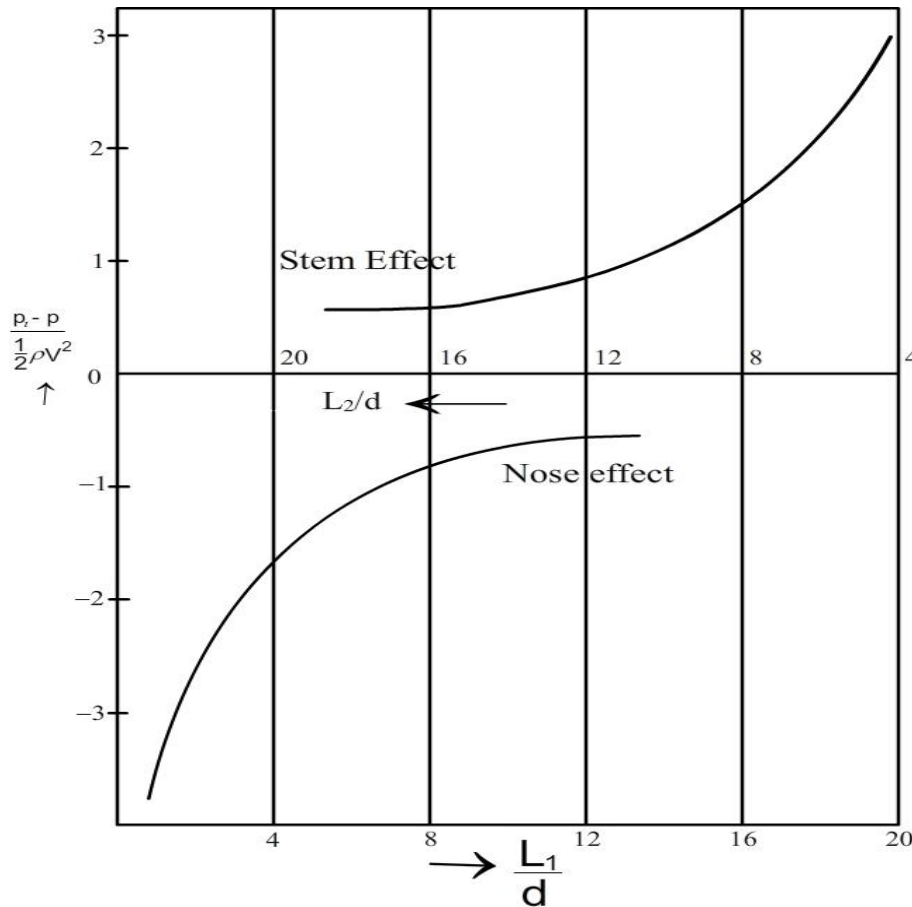


Fig.5.20 The nose and stem effects in a Prandtl tube

Because of the intrusive nature of the probe, the flow will be accelerated by the nose. The effect will be to reduce the static pressure which is called the nose effect. In contrast, the effect of stem will be to locally stagnate the flow and thereby to increase the static pressure. This

effect is the stem effect. As shown in the Fig.5.20, the position of the orifices are so chosen that the two effects neutralize each other. Additionally the probe must be slender (say ~ 1.0 to 1.5mm dia) and kept parallel to the flow.

5.8.3 Static pressure probes for supersonic flow

When Mach number is more than 1.0, shock appears. When the cone angle of the probe is less than the shock detachment angle for the given Mach number [shown in Fig.5.23] and if the orifices are located well downstream of the shock wave, the measured static pressure will tend towards the value for the undisturbed flow. Conical or ogival shaped tubes are used.

Probes are made small and with static taps on the cone surface. The effect of yaw is reduced by arranging several orifices so that the pressure inside the tube is an average value. Usually the tube has 4 to 8 orifices whose diameter is about $1/10$ th of the outside diameter of the tube.

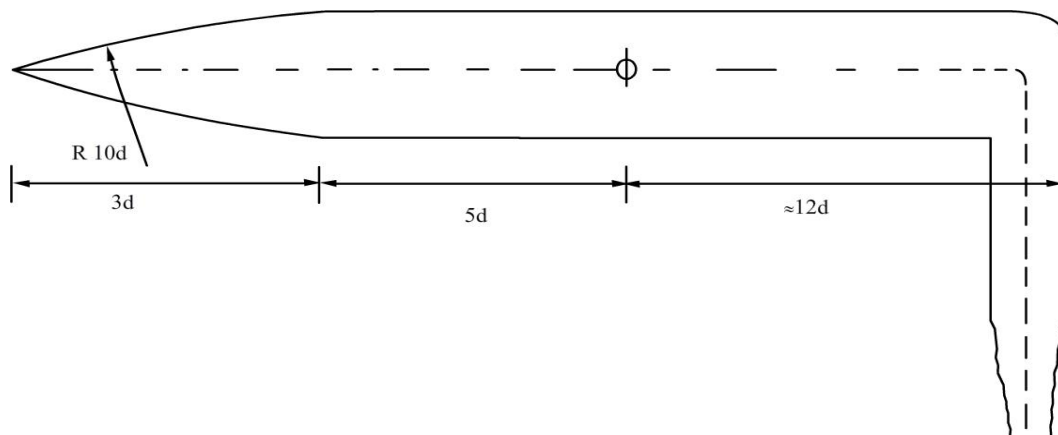


Fig.5.21 Ogival shaped static pressure probe for supersonic flow

Good results are obtained with ogival tubes. The tube shown in Fig.5.21 has a systematic error within 1%. Angle of the cone should be less than the angle at which the shock wave becomes detached from the cone. The error in the measurement of static pressure decreases as the distance of the orifice from the tip of the probe increases.

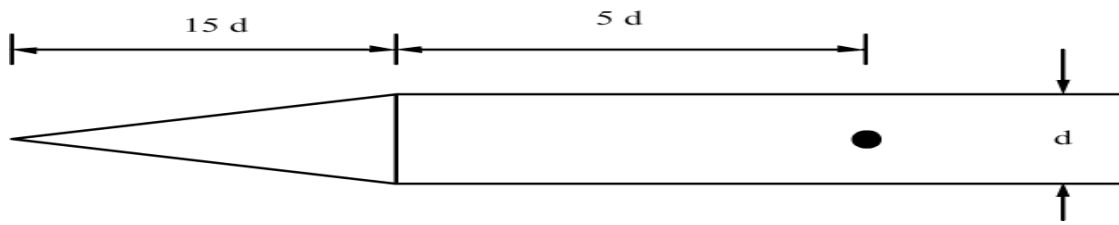


Fig.5.22 Conical static pressure probe for supersonic flow

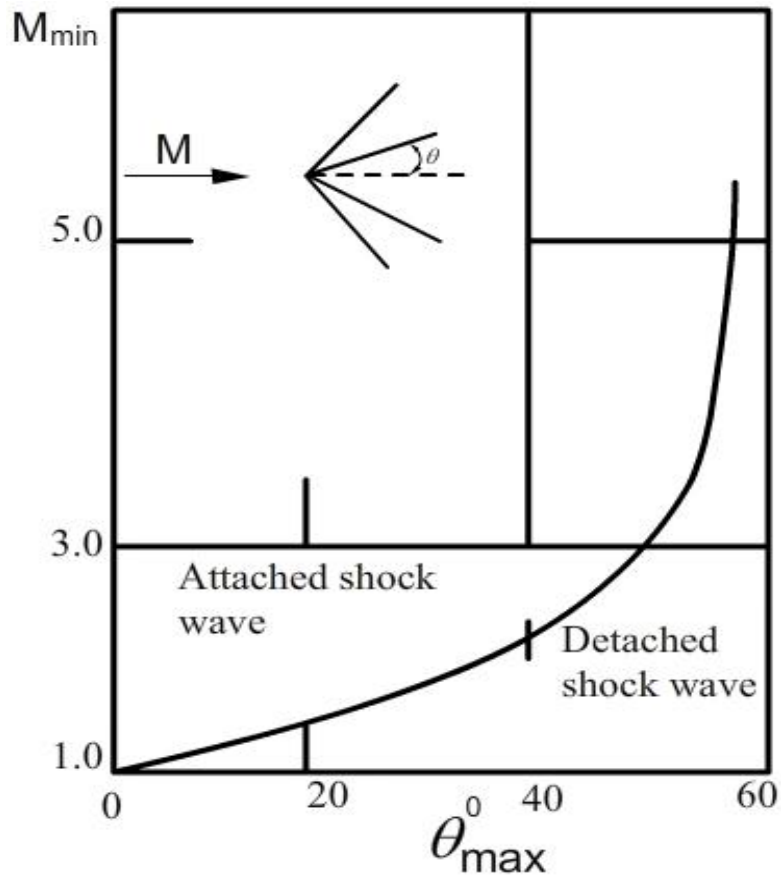


Fig.5.23 Maximum deflection angle for different Mach numbers

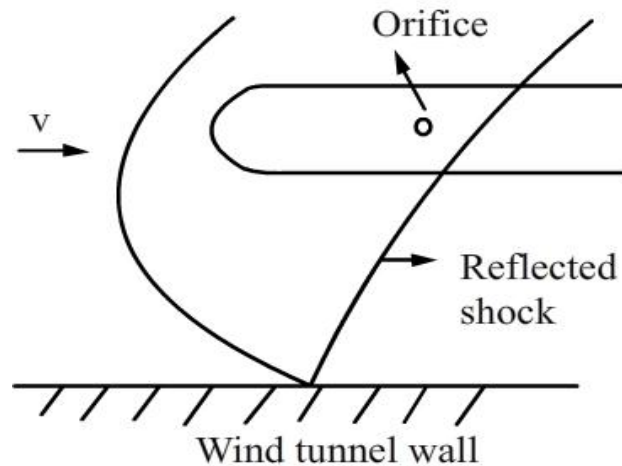


Fig.5.24 Reflection of the shock from the wall

It is important to have long pointed tubes. Otherwise there is the possibility that the reflected shock may affect the static pressure readings. Roughness at the edges of the orifices too may cause large errors in measurement.

5.10 Measurement of stagnation or total pressure

5.9.1 Insubsonic flows

The gas particles come to rest so quickly at the stagnation point of a body, that heat transfer and friction losses are negligible. Therefore, in subsonic flows only isentropic changes occur. Hence the stagnation pressure measured in a subsonic flow is not significantly different from that in the settling chamber. Total pressure is measured with a Pitot tube which a cylindrical tube is having an orifice pointing towards the flow. Axis of tube must coincide with the flow direction. It is a practice to use tubes which generally have blunt ends.

Such tubes are insensitive to yaw upto ± 10 to 12°

The relation between the stagnation pressure measured and the static pressure may be expressed as follows:

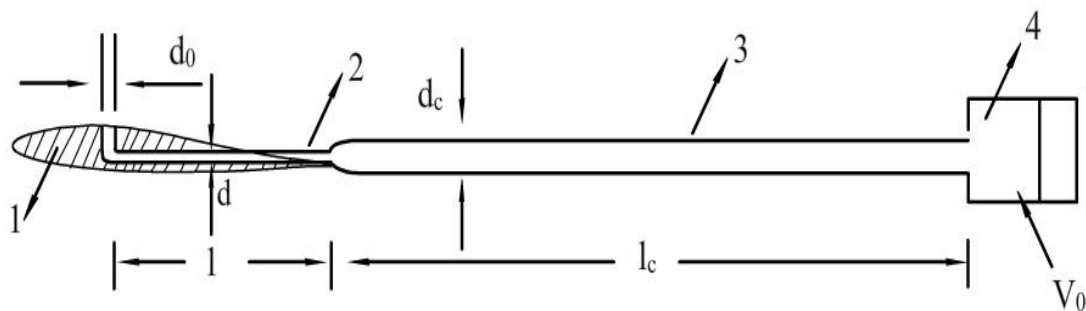
$$\frac{p}{p_0} = \left(1 + \frac{\gamma - 1}{2} M^2 \right)^{\frac{\gamma}{\gamma - 1}}$$

where p_0 is the total pressure and p the static pressure.

5.9.2 Insupersonic velocities

Shockwave appears upstream of the tube nose. Therefore tube measures only pressure behind the shock wave. Normal shock equations give the relation between the total pressures upstream and downstream of the shock. As the bow shock formed in front of the Pitot tube has the normal part only in the central region, the tube diameter for measurements in supersonic flow is usually kept very small.

5.10 Lag in manometric systems



1 - model 2 - capillary tube 3 - connecting tube

4 - air space of sensing element of manometer

Fig.5.25 Wind tunnel model with the manometric system

When the pressure changes near the orifice which is connected to a manometer, equilibrium in the manometer is established not immediately but after a certain time. If the pressure is read of earlier there will be gross errors.

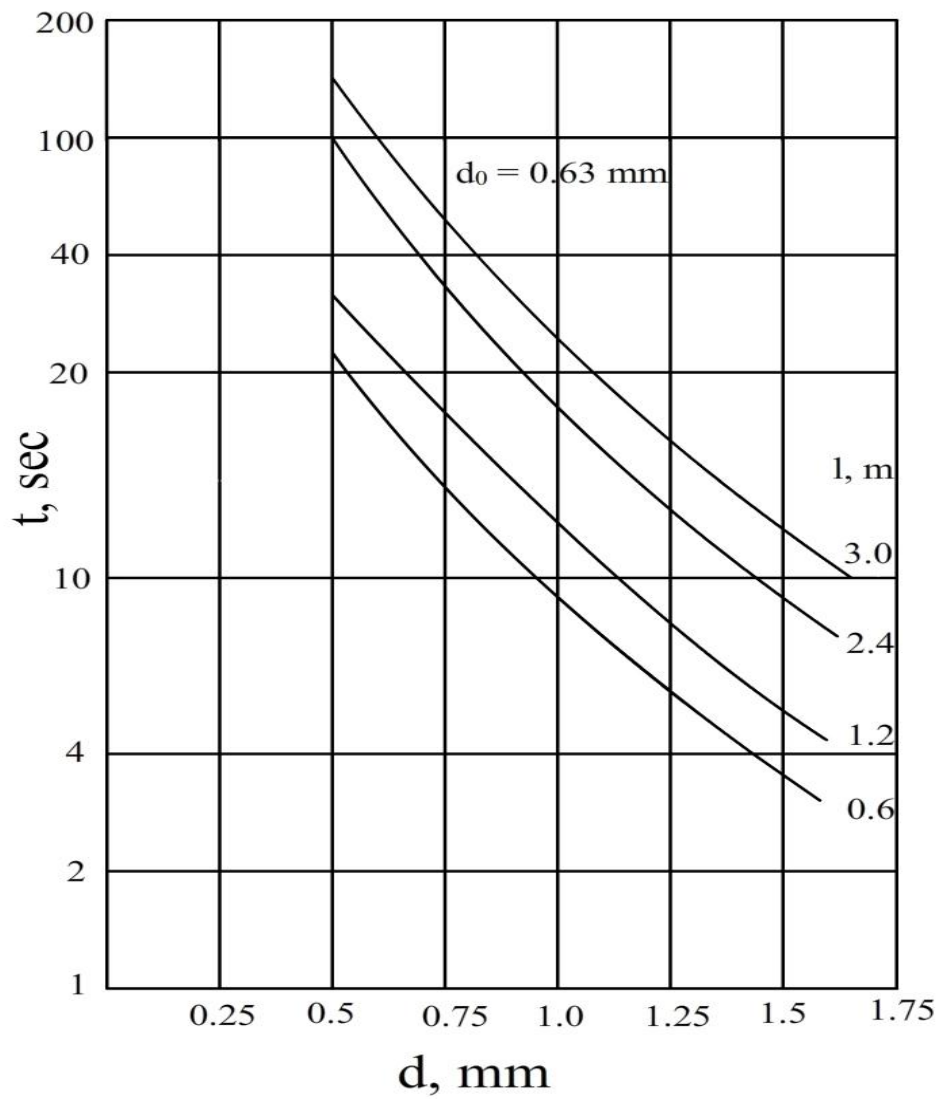


Fig.5.26 Transmission lag as a function of capillary diameter

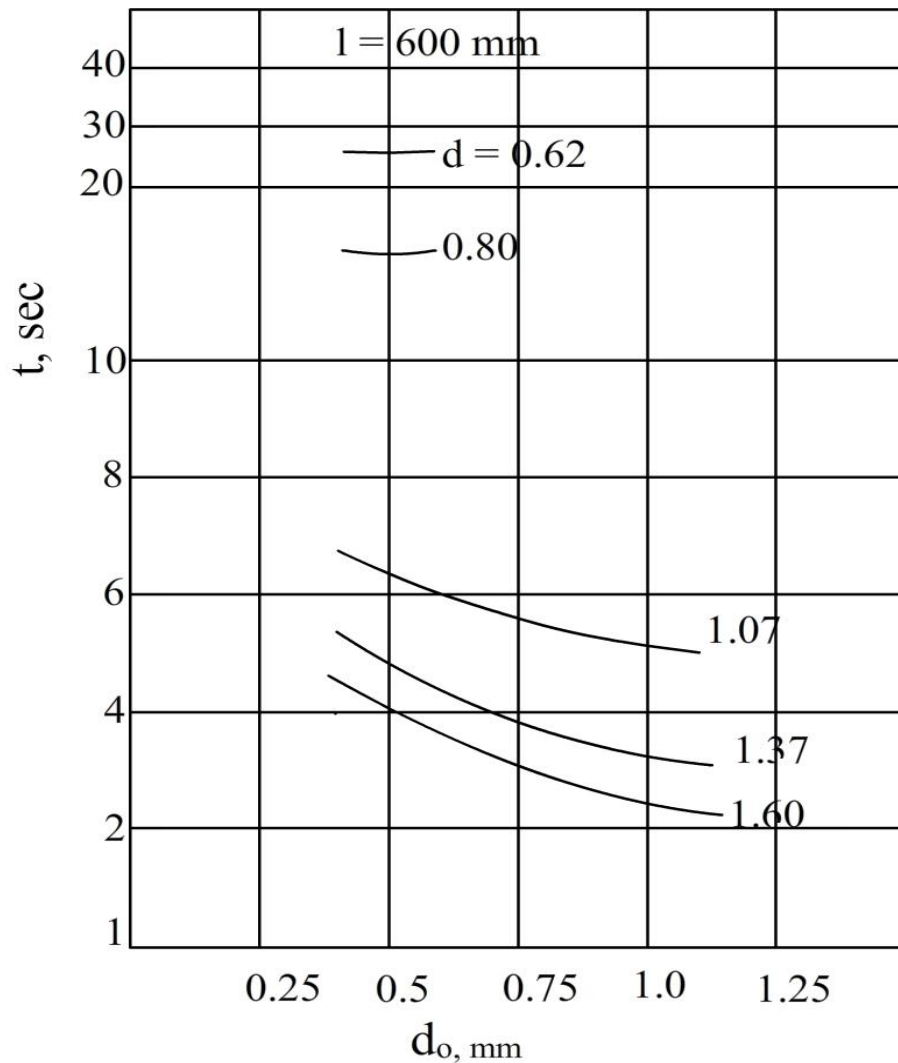


Fig.5.c Transmission lag as a function of orifice diameter

Smaller transmission lags are necessary not only for high reliability but also for reducing the duration of experiments. Equilibrium will be established in the manometric system later after the pressure on the model is stabilized. The run times should be longer than the transmission lag.

Transmission lag is caused by:

- a) Resistance of the tubes
- b) The change in air density
- c) and inertia of the moving masses

The main factors influencing the transmission lag are the orifice diameter d_o , the diameter d of the capillary and d_c of the connecting tube and their respective lengths l and l_c .

The orifice diameter is of small influence when $d/d_0 < 2.5$. When $d/d_0 > 2.5$ the transmission lag increases sharply. The orifice diameter should not be less than half the diameter of the capillary tube. The influence of the diameter of the capillary tube is very strong. A reduction of this diameter has its main effect an increase in the resistance to the flow of gas. An increase in the length of the capillary tube has a significant effect on the lag. Capillary tubes should have larger diameter and shorter length.
